WESTERN POWER DISTRIBUTION

INNOVATION

NEXT GENERATION NETWORKS

# Harmonic mitigation

## Literature Review

| | | |
|---|---|---|
| Report Title | : | Harmonic Mitigation Literature Review |
| Report Status | : | Approved |
| Project Ref | : | WPD NIA 043 Harmonic Mitigation |
| Date | : | 27/01/2020. |

**Document Control**

| | Name | Date |
|---|---|---|
| Prepared by: | Atheer Habash and Grazia Todeschini (Swansea University) | 15/11/2019 |
| Reviewed by: | Zia Emin (PSC) | 28/11/2019 |
| Approved (WPD): | Chris Harrap (WPD) | 27/01/2020 |

**Revision History**

| Date | Issue | Status |
|---|---|---|
| 15/11/2019 | 0.1 – 0.5 | Drafts |
| 27/01/2020 | 1.0 | First issue |

## Contents

## Glossary

| Abbreviation | Term |
|---|---|
| AF | Active filter |
| ANF | Adaptive notch filter |
| ANN | Artificial neural network |
| CF | Compact fluorescent |
| DFT | Discrete Fourier transform |
| DPWM | Discontinuous pulse-width modulation |
| DSRF | Double synchronous reference frame |
| DVR | Dynamic voltage restorer |
| EMC | Electromagnetic compatibility |
| EMI | Electromagnetic interference |
| FFT | Fast Fourier transform |
| FPGA | Field-programmable gate array |
| HP | High pass |
| IP | Insulation protection |
| LP | Low pass |
| MAF | Multistage adaptive filter |
| MMCC | Modular multilevel cascaded converters |
| MPPT | Maximum power point tracking |
| NLL | Non-linear load |
| NSRF | Negative-sequence reference frame |
| PF | Passive Filter |
| PCC | Point of common coupling |
| PI | Proportional-integral |
| PLL | Phase-locked loop |
| PSRF | Positive-sequence reference frame |
| PV | Photovoltaic |
| PWM | Pulse-width modulation |
| RDFT | Recursive discrete Fourier transform |
| RTC | Real-time controller |
| RES | Renewable energy source |
| SCL | Short circuit level |

| | |
|---|---|
| SFX | Synchronized filtered-x |
| SM | Sub-module |
| SMPS | Switch mode power supply |
| SPWM | Sinusoidal pulse-width modulation |
| SRF | Synchronous rotating frame |
| SVPWM/SVM | Space vector pulse-width modulation/ Space vector modulation |
| THD | Total harmonic distortion |
| THIPWM | Third harmonic injection pulse width modulation |
| UPQC | Unified power quality conditioner |
| WT | Wavelet transform |

# 1 Executive Summary

This literature review addresses how distribution network connected inverters associated with renewable energy sources may provide harmonic compensation as an additional, or "ancillary service". In other words, how inverters may be used as Active Filters while simultaneously delivering fundamental power.

Current harmonics are caused by nonlinear devices connected to the power grid as they draw or inject non-sinusoidal currents when supplied with a sinusoidal voltage. These current harmonics interact with the power grid's impedance to create voltage distortion that can adversely affect the distribution system's equipment, and customer equipment that is connected to the system. Power quality standards have been developed for the UK system (currently G5/4-1, with G5/5 expected to be implemented during 2020) that define voltage distortion planning levels. Newly connected equipment is expected to be compliant.

Mitigation of harmonics produced by connected non-linear equipment, loads or generation, can be achieved by installing either Passive Filters (combinations of inductive, capacitive and resistive components that sink the harmonic currents) or Active Filters (power converters controlled to inject current harmonics with opposing phase angles). Active Filters can either be standalone systems, or can be implemented as additional control algorithms placed within an existing power converter (the focus of this WPD innovation project).

The main functional blocks required within an Active Filter controller are: harmonic current or voltage extraction to establish harmonic levels; a current loop controller to establish the required level of intervention; and gate signal generation to implement the required electrical intervention. This review details different implementations for each of these main functional blocks, together with advantages and disadvantages of each implementation.

The review also identifies previous work that has investigated power converter controller implementations that deliver both fundamental power and harmonic mitigation. In these cases, active filtering is performed as an 'ancillary service'. Three specific implementation examples are described in detail, together with simulation results. Each simulation shows the feasibility of mitigating harmonics and also illustrates: (i) the requirement to limit harmonic mitigation in coordination with fundamental power output, to operate the power converter within equipment ratings; and (ii) the ability of mitigating time-varying harmonics.

Results from hardware implementations of Active Filter operation within multi-functional inverters are not very common in the literature, partly due to the novelty of this approach. However, two examples are presented that again show successful mitigation of harmonics (one with additional phase balancing functionality, and one for a hybrid wind–PV system). One further example is also presented where harmonic mitigation functionality was added to a STATCOM operating in south-west Scotland on a system that was experiencing voltage total harmonic distortion (THD) of up to 3.3%. With active filter functionality enabled, voltage THD was successfully reduced to around 1%.

This literature review has provided a detailed summary of previous research and development that can beneficially be built upon in the work Swansea University are undertaking to develop an algorithm that can improve the network's harmonic levels by controlling existing Distributed Generation inverters, acting individually or as a coordinated group.

# 2 Introduction

It is expected that due to the increasing number of non-linear devices being connected to the distribution network, the harmonics in the network can become a challenge for Distribution Network Operators (DNOs). One of the most common solutions to mitigate harmonics consists in installing harmonic filters. These devices are designed to absorb a well-defined band of harmonics by providing a low-impedance path for certain frequencies but they are not effective under all operating conditions.

An Active Filter (AF) is an alternative solution to mitigate excessive harmonic levels in the distribution system and it consists of a power converter controlled to absorb harmonic components [1]. A more detailed description of AF operation, and several applications are described in Section 4 and Section 5. AFs, however, are not commonly used at the distribution system level, due to the cost of this technology. An overview of AF applications and comparison of the cost between AF and Passive Filters (PF) are presented in Section 6.

More recently, there has been a renewed interest in the use of AFs, given that this feature can be provided as an 'ancillary service' [2], [3]. In other words, AF can be performed in addition to other control functionality within the power converters [4]. This approach allows using the same power converter unit to provide additional services depending on grid conditions, thus reducing the number of devices installed. Section 7 will describe the state-of-the art in the use of AF as ancillary service.

The Harmonic Mitigation project proposes that AF functionality could be added to a photovoltaic (PV) inverter[1], while still allowing for fundamental power flow. This application will be studied for the Tiverton 33 kV Network. More details of the area under study will be provided in and Section 8.

## 2.1 Project structure

This innovation project is structured in four work packages; each work package is briefly summarised below.

**WP1: Model Creation and Base Studies**

The first work package consists mainly of two parts. The first is to perform a comprehensive literature review to explain existing applications of AF, their costs, and the unique contributions of this project. The results of the literature review will be presented in this report.
The second part consists in modelling and validating a Simulink model of the Tiverton substation and surrounding feeders, including three solar farms. The Simulink model will be based on an existing model developed in DIgSILENT PowerFactory.

[1] In this document, the term 'inverter' is used to describe power electronics devices used to convert dc power to ac power, such as in the case of PV inverters, where the power flow is unidirectional from the PV panel to the ac grid. The more generic term 'power converter' will be used when power electronics devices are used for bi-directional power flow, or when the power flow direction is not specified.

More details about the model development will be described in Section 8.

**WP2: Algorithm design, development and implementation for single inverter control**

The second work package consists in developing a control algorithm that allows the PV inverter to perform AF operation. This work package focuses on developing this functionality for an individual unit.

The amplitude and frequency of harmonic components injected by the PV inverter will depend on two factors: the amount of fundamental power extracted from the PV panels, and the harmonic levels existing in the grid.

The proposed algorithm will not affect the fundamental power flow, but it will be added as parallel control functionality. If the inverter in injecting full power, and therefore the full rated current is flowing through the switches, a mechanism is put in place to block harmonic injection and avoid inverter overload. On the contrary, if the inverter is operating below the rated power, harmonic injection is allowed and therefore the proposed algorithm is activated. The inverter loading is continuously verified by the algorithm, to ensure that the ratings are not exceeded.

**WP3: Algorithm design, development and implementation for multiple inverter control**

This work package will extend the control algorithm developed in WP2 to multiple inverters. This work package will be divided into two parts.

In the first part, each inverter unit will be controlled as AF independently. This means that there is no coordination or communication between the inverters. The improvement of harmonic levels across the Tiverton Network will be then assessed and compared with the levels measured in WP1.

In the second part of this work package, a coordinated control between different inverters will be developed, to optimise harmonic injection based on the source of harmonic currents, and on the power injected by each power converter.

**WP4: Hardware in the Loop (HiL) testing**

Experimental validation of the control will be carried out in the Swansea University power electronics laboratory. This laboratory currently has a facility to test only one power converter. The network model will be developed in OPAL-RT and the control will be developed using D-SPACE.

The output of the power converter will be monitored using a power quality meter to verify the harmonics. The operation will be compared with the results from Work Package 2.

The final report will help quantifying the benefit of the proposed application for Western Power Distribution and other DNOs, the commercial value of it, and the next steps leading to implementation.

# 3 Harmonic issues on distribution systems

## 3.1 Introduction to harmonics

Harmonics[2] are caused by nonlinear loads connected to the power grid. Non-linear loads draw non-sinusoidal currents when supplied with a sinusoidal voltage, and therefore they introduce harmonic components to the fundamental frequency.

Several types of non-linear loads exist, as shown in Table 1 [5]. In the modern power grid, the main sources of harmonics are power converters, with power ratings from 1000s MW for HVDC applications, to 75 W for household appliances, such as televisions. Renewable energy sources (RESs) such as wind turbines and solar panels are connected to the power grid by means of power converters, and they have been contributing to increased harmonic levels in the grid. Other non-linear sources of harmonics include arcing devices, fluorescent and high intensity discharge lights.

Table 1: Overview of harmonic sources, listed per type of equipment.

| Category | Connection | Format | Loads |
|---|---|---|---|
| Utility equipment (large size) | Three-phase | HVDC converters and FACTs | Transformers, static compensators |
| Industrial (large size) | Three-phase | | AC Motors, Arc Welders, Electric arc furnaces, Induction Heaters, |
| Commercial (medium size) | Three-phase delta-connected | Power converters for photovoltaic and wind generation, Electric vehicles | SMPS, variable speed/frequency drives, heat pumps |
| Residential (small size) | Single phase | Power converters for photovoltaic generation, Electric vehicles | SMPS, CF Light, LED Light |
| Note: Capacitor banks are not source of harmonics, but may contribute to harmonic amplification by changing the system frequency response | | | |

Due to voltage drop across the line impedances, harmonic currents lead to voltage harmonic distortion at the load bus, as shown schematically in Figure 1. As a consequence, other devices connected to the same bus will be subject to voltage distortion, and they will draw non-sinusoidal current. It is clear therefore that harmonics spread very easily within the distribution system and affect all equipment connected to the grid. More importantly, it is difficult to identify the source of harmonics when multiple loads are present in the system.

[2] In this report, the term 'harmonics' refers to waveform components with frequency that is an integer multiple of the fundamental component. This is to be consistent with the standards that provide limits for integer harmonics and calculate the THD taking into account integer harmonics only.

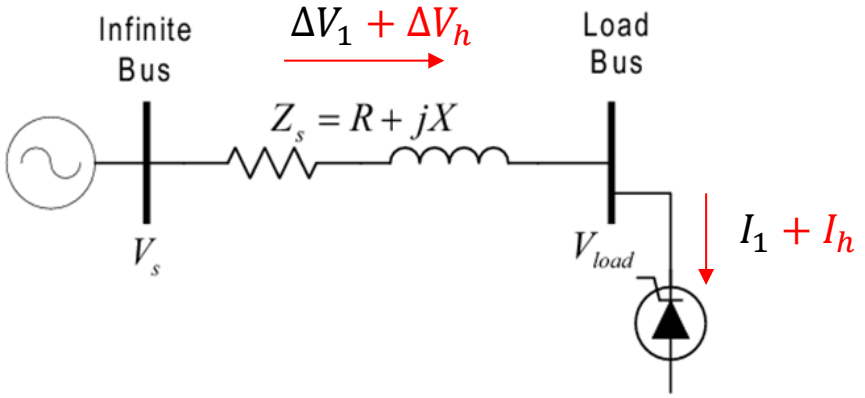


Figure 1: Illustration of harmonic voltage drop across a feeder, and harmonic distortion at the load bus.

When harmonic levels are within prescribed planning levels, it is deemed that there will be electromagnetic compatibility between the electricity supply system and customer's connected equipment and therefore no harmonic mitigation is required. Increasing level of harmonics result in the following detrimental effects:

- Deterioration of power factor correction capacitor banks due to overloading.
- Additional losses in electrical machines, transformers and conductors. On the short term, this causes a reduced efficiency. In the long term, it may lead to reduction of equipment lifetime.
- Errors in measurements when standard instrumentation is used.
- Telephone interference.
- Tripping of protective devices.
- Failure of equipment.

To eliminate these drawbacks and improve the power quality and total harmonic distortions, power quality standards have been developed to define a framework for harmonic control and electromagnetic compatibility (EMC) between devices.

## 3.2 Standards for limitation of harmonics

Power quality standards have been developed to provide a platform between planning, compatibility, emission and immunity levels so that they can function in a coordinated way. Emission limits are a result of that coordination and they appropriately minimise harmonic propagation in the power grid. The UK has been pioneering this process as evidenced by a series of G5/x publications [6].

Nowadays, different standardization bodies in the world have developed power quality standards: the most well-known are [7] and [8] which are applied in numerous countries, including North America, Europe, the Middle East and Asia.

To take into account the characteristics of the UK power grid, the Energy Networks Association in 2001 has published the Engineering Recommendation (ER) G5/4 listing the UK harmonic distortion limits. Later on, in 2005, the revision G5/4-1 was issued [9] with minor approach changes in some parts of the G5/4 document. This standard, when possible, reflects the IEC recommendations, however, it includes additional provisions for conditions that are specific to the UK, such as for example the assessment procedures for connection of non-linear equipment.

The recommendation sets planning levels for harmonic voltage distortion to be used while connecting non-linear equipment in order to limit the level of individual harmonics and the total harmonic distortion (THD). Table 2 shows the THD planning levels as a function of the nominal system voltage. Table 3 and Table 4 show the planning levels for individual harmonic voltage components for two different sets of system voltages. These tables are included because they provide planning levels for the system under consideration in this research project. Additional tables and limits are can be found in [9].

Compliance with G5/4-1 requirements is part of the grid connection process in the presence of non-linear equipment and is actively managed by the host networks in the UK [10].

Table 2: THD planning levels according to [9].

| Voltage Level | THD Level |
|---|---|
| 400 V | 5% |
| 6.6 kV, 11 kV and 20 kV | 4% |
| 22 kV to 400 kV | 3% |

Table 3: Planning levels for harmonic voltages in systems with 6.6 kV, 11 kV and 20 kV [9].

| Odd harmonics | | Odd harmonics | | Even harmonics | |
|---|---|---|---|---|---|
| Order | Level (%) | Order | Level (%) | Order | Level (%) |
| 5 | 3.0 | 3 | 3.0 | 2 | 1.5 |
| 7 | 3.0 | 9 | 1.2 | 4 | 1.0 |
| 11 | 2.0 | 15 | 0.3 | 6 | 0.5 |
| 13 | 2.0 | 21 | 0.2 | 8 | 0.4 |
| 17 | 1.6 | >21 | 0.2 | 10 | 0.4 |
| 19 | 1.2 | | | 12 | 0.2 |
| 23 | 1.2 | | | >12 | 0.2 |
| 25 | 0.7 | | | | |
| >25 | 0.2+0.5(25/h) | | | | |

Table 4: Planning levels for harmonic voltages in systems with >20 kV and <145 kV [9].

| Odd harmonics | | Odd harmonics | | Even harmonics | |
|---|---|---|---|---|---|
| Order | Level (%) | Order | Level (%) | Order | Level (%) |
| 5 | 2.0 | 3 | 2.0 | 2 | 1.0 |
| 7 | 2.0 | 9 | 1.0 | 4 | 0.8 |
| 11 | 1.5 | 15 | 0.3 | 6 | 0.5 |
| 13 | 1.5 | 21 | 0.2 | 8 | 0.4 |
| 17 | 1.0 | >21 | 0.2 | 10 | 0.4 |
| 19 | 1.0 | | | 12 | 0.2 |
| 23 | 0.7 | | | >12 | 0.2 |
| 25 | 0.7 | | | | |
| >25 | 0.2+0.5(25/h) | | | | |

The harmonic standard [9] has been further revised and the new version G5/5 will become applicable in 2020.

Ensuring that voltage harmonic levels are controlled is important to ensure that system power quality is maintained. When harmonic levels exceed the values provided in the relevant standards, harmonic mitigating solutions are required.

The most common harmonic mitigating solutions will be described in the next section.

# 4 Harmonic mitigation approaches

When harmonic limits are exceeded, different mitigating solutions can be implemented. The first approach to mitigation is to identify loads that are not compliant and cause excessive harmonic distortion in the system. If this task is successful, the offending load will be required to correct the excessive injection at the customer premises. In some cases, for example with power converters, a retrofitting of the control algorithm may result in reduced harmonic distortion.

If this this not possible, then a solution at the system level is required. This solution will consist of connecting an external device to mitigate the harmonics. This device is known as 'power filter'.

An overview of the power filter topologies is provided in Figure 2. The main distinction is between passive filters and active filters [11]. Within these two families, several different types of filters exist. The most common topologies of power filters will be described in the next sections.

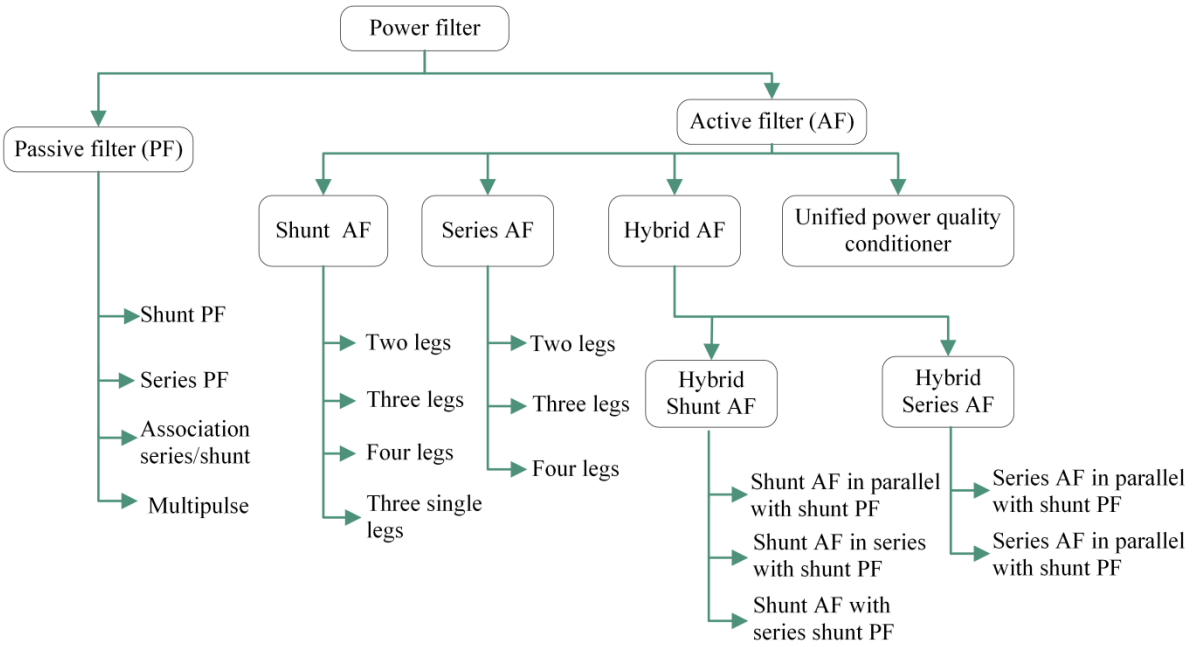


Figure 2: Classification of power filters topology used for power quality improvement [12].

## 4.1 Passive filters

Passive filters are the most commonly used mitigating solutions for harmonic concerns. They consist of inductances, capacitances, and/or resistors configured and tuned in a way to provide a low-impedance path for harmonic currents [5].

The most common passive filter configurations will be shortly outlined in the next sections.

### 4.1.1 Single-tuned (or resonant) filter

The single-tuned filter is one of the most common and economical type of passive filter. The single-line diagram of the single-tuned filter connected to the point of common-coupling (PCC) of a simple network is shown in Figure 3: this filter is composed of an inductor $L$ connected in series with a capacitor $C$. Damping may be provided by choosing a reactor with an adequate quality factor, or by adding a separate resistor – the resistive element is not shown in Figure 3 because generally for this type of filter it is very small.

The values of inductance and capacitance are calculated in accordance with the harmonic frequency to be eliminated:

$$f_n = \frac{1}{2\pi\sqrt{LC}} \tag{1}$$

where $f_n$ is the tuning frequency. At the tuning frequency, the filter impedance is equal to the series resistance, that generally is very small, and therefore harmonic currents at this frequency are directed to earth. Figure 4 presents an example of frequency response for a single-tuned filter: the first graph shows the impedance magnitude and the second graph shows the phase angle. The minimum impedance magnitude is obtained at the resonant frequency $f_n$. The phase angle indicates capacitive behaviour for frequencies below $f_n$, and inductive behavior with increasing frequency.

A single-tuned filter is required for each harmonic component to be eliminated. In the case of multiple harmonics to be eliminated, more than one filter is required. The use of two single-tuned filters can be replaced by a double-tuned filter, as shown in the next section.

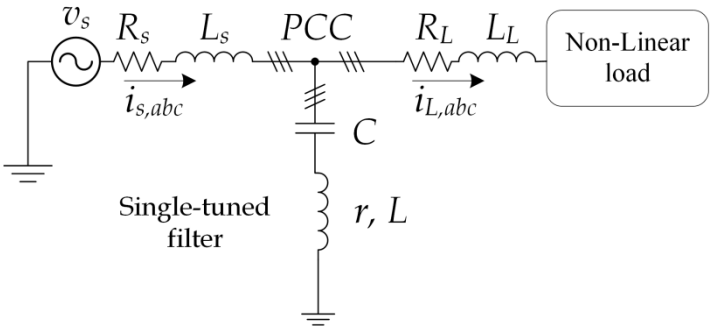


Figure 3: Single-tuned filter configuration: the filter parameters are $C$, $L$ and $r$. The grid is represented by a Thevenin equivalent ($v_s$, $R_s$, $L_s$), while a non-linear load is connected to the PCC by means of a resistance $R_L$ and inductance $L_L$.

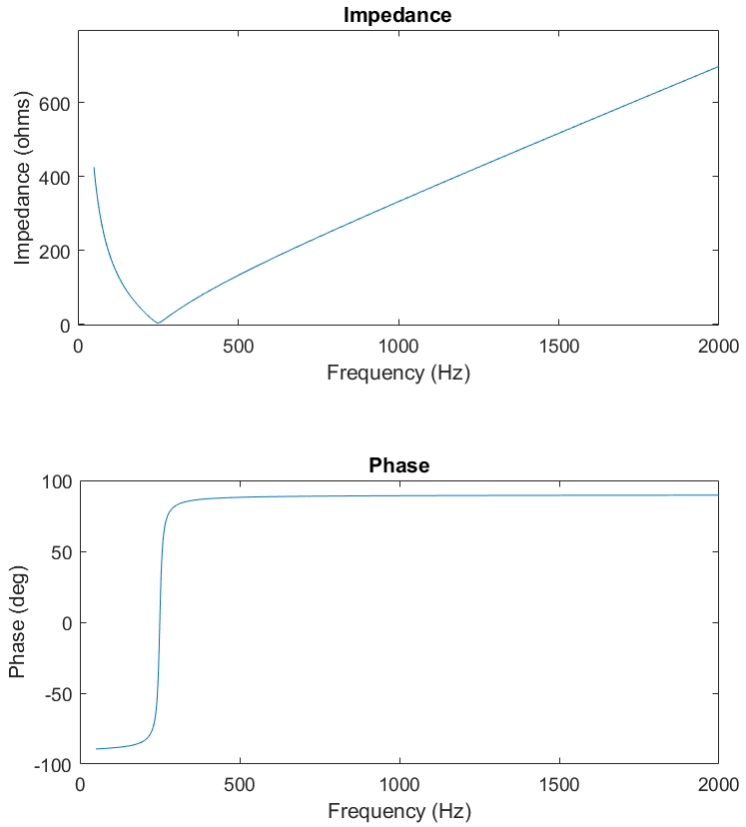


**Figure 4: Frequency response for a single-tuned passive filter. The tuning frequency $f_n$ is 250 Hz. The top graph shows the impedance magnitude, the second graph shows the phase as function of the frequency.**

### 4.1.2 Double-tuned filter

The impedance of two single-tuned filters near the resonant frequency is equivalent to the impedance of a double-tuned filter. The single-line diagram of the two solutions is shown in Figure 5. Figure 6 shows the frequency response of the double-tuned filter: the behaviour is similar to the one described for the single-tuned filter, and the main difference is that the equivalent impedance has to 'minimum' points, corresponding to the two tuning frequencies.

The correlation between the values of the filter components is provided in [5]. The double tuned filter reduces the power loss at the fundamental component, and reduces the number of inductors to be subject to the full line impulse voltage. Therefore, the main applications of the double-tuned filter are found at high-voltage levels, in particular for line commutated converter HVdc applications [13].

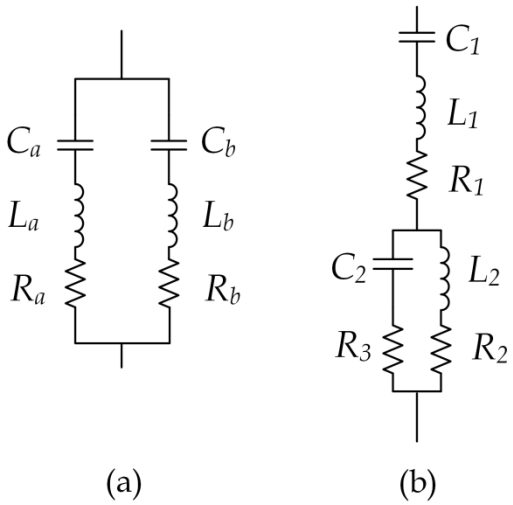


Figure 5: Comparison between (a) two single-tuned filters and (b) a double-tuned filter.

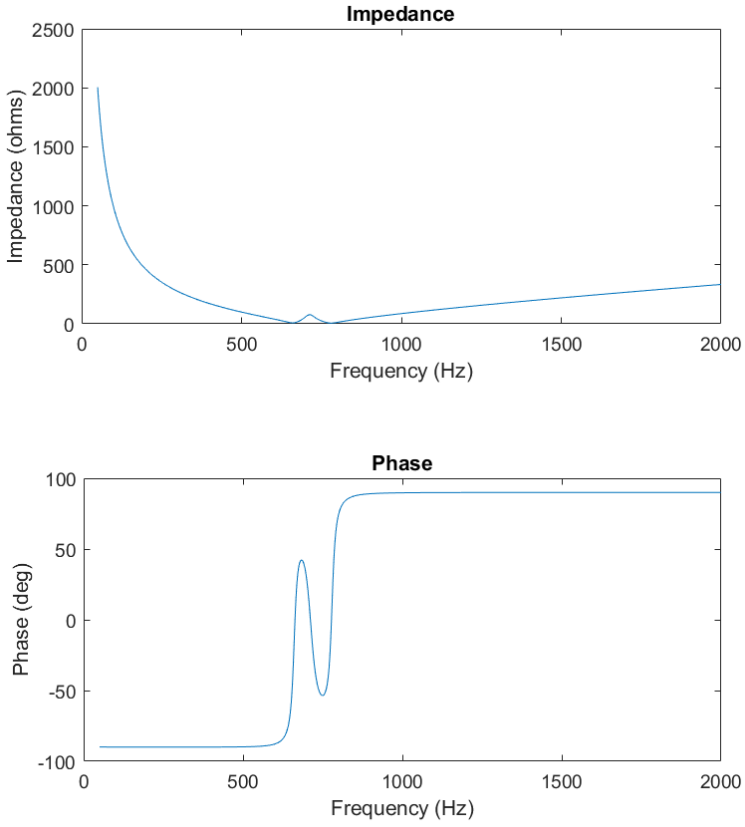


Figure 6: Frequency response for a double-tuned passive filter. The tuning frequency is 250 Hz. The top graph shows the impedance magnitude, the second graph shows the phase as function of the frequency.

### 4.1.3 Damped (or high-pass) filter

The damped (or high-pass filter) provides a low impedance for a wide spectrum of harmonics without the need to use multiple parallel branches. Additionally, its performance and loading are less sensitive to temperature variations, frequency variations and component tolerances. However, it generally requires higher rating and it is characterised by higher losses.

Among damped filters, several configurations are possible: first-order, second-order, third-order and C-type [5]. The second-order damped filter is the most common configuration, and the single-line diagram is shown in Figure 7. The frequency response is shown in Figure 8: in this case, one can notice that the impedance has a minimum point at the tuning frequency, and then the frequency response is flat for increasing frequencies, thus allowing the elimination of a broad range of harmonics.

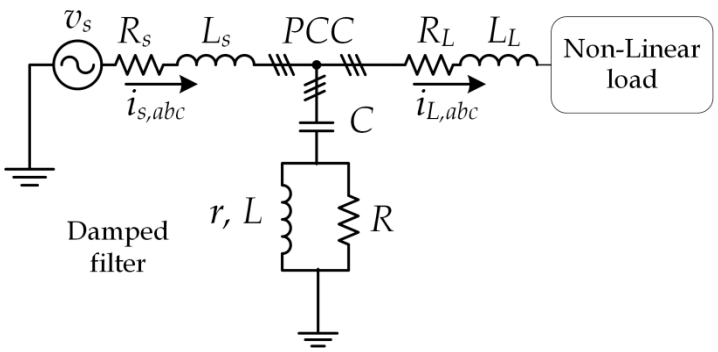


Figure 7: Modification of the system shown in Figure 3 to include a second-order damped filter.

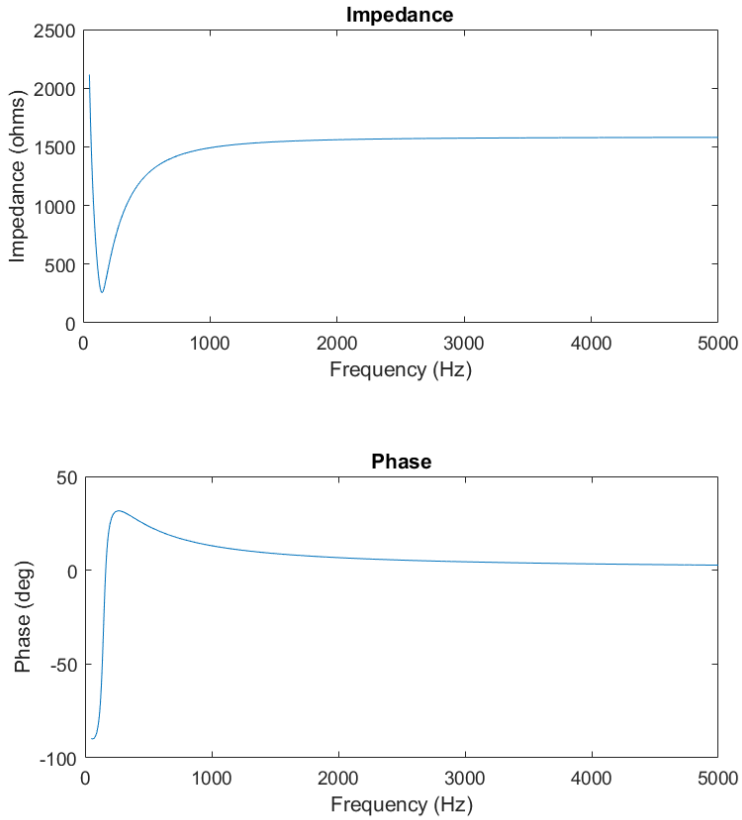


Figure 8: Frequency response for a damped passive filter. The tuning frequency is 150 Hz. The top graph shows the impedance magnitude, the second graph shows the phase as function of the frequency.

### 4.1.4 Resonant Damped Filter

These filters are composed of resonant filters for specific harmonic ranges, connected in parallel with high pass filter to eliminate the higher harmonics.

Figure 9 shows the connection of two single-tuned resonant filter for 5th and 7th harmonics with a high-pass filter. This configuration allows for mitigating a broad spectrum of harmonic frequencies, however, it requires a high number of components. The frequency response is similar to the one shown in Figure 8.

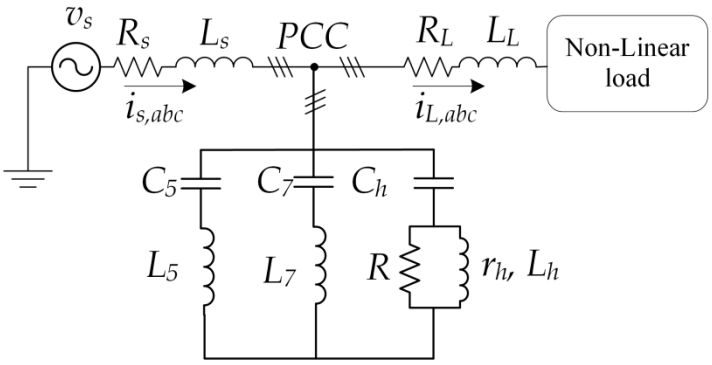


Figure 9: Modification of the system shown in Figure 3 to include a resonant damped filter.

### 4.1.5 Other passive filters types

**Series passive filters**

A series-passive solution can be achieved using a line reactor. This device is commonly used in front of power converters. A line reactor provides a low cost way to reduce current harmonics, whilst adding a level of protection to the power converter. A typical 3% input choke can reduce the harmonic current distortion for a PWM-based drives from approximately 80% to 40%, as shown in Figure 10 [14].

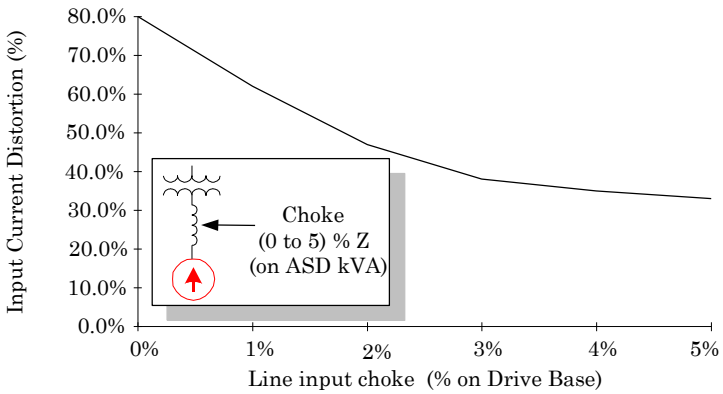


Figure 10: Effect of adding a line choke to the input current of a power converter [14].

The inductance slows the rate at which the capacitor on the dc bus can be charged and forces the drive to draw current over a longer time period. The net effect is a lower-magnitude current with much less harmonic content while still delivering the same energy

The next option is to use a series harmonic filter consisting of a parallel inductor and capacitor which present a large impedance to the relevant frequency [5]. It provides more effective compensation than a line choke, significantly reducing total harmonic distortion (THD).

Other configurations are theoretically, possible, however, series passive filters need to be rated for the full line current at fundamental frequency. Therefore, they are not as common as shunt filters. However, series active filters exist and they will be described in Section 0.

**Multi-pulse filters**

A commonly used series-passive solution is a multi-pulse filter, consisting of a multi-winding transformer with phase shift in the windings. An example of such configuration is shown in Figure 11 for the case of 6-pulse converters. The transformer windings are delta-delta connected for the first converter, and delta-wye connected for the second one. Because every secondary winding has its own rectifier, a six-pulse configuration can target and effectively cancel out the $5^{th}$,$7^{th}$, $11^{th}$ and $13^{th}$ harmonics.

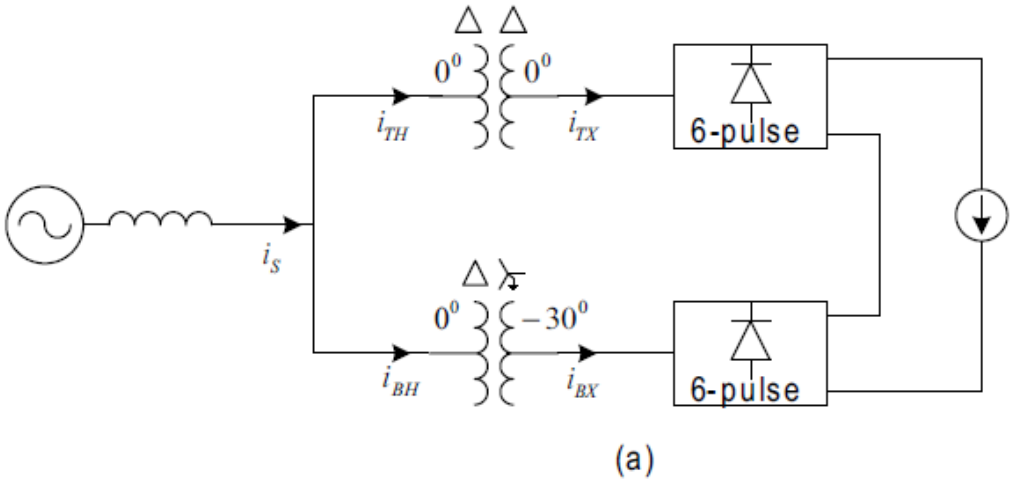


Figure 11: Example of transformer configuration used to mitigate harmonics from multi-pulse converters.

The downside of using multi-pulse filters is that they are very sensitive to voltage unbalance. On an 18-pulse drive under 50% load, when the unbalance is increased from 0% to 3%, the current THD increases from 10% to 35%.

When using multi-pulse filters, consideration needs to be given to planning the drive system and deployment as units are often large, heavy and difficult to retrofit [5].

### 4.1.6 Discussion on passive filters

Passive filters benefit from a simple structure and relatively low cost, and they have been used successfully by utilities worldwide to manage harmonics and they are very suitable for many applications.

However, they present some drawbacks and limitations. For example, detuning – i.e. deviation from the nominal tuning frequency, reduces the effectiveness of the filter. This effect is due to various factors: variation of system operating frequency, aging of capacitor or inductors, effect of temperature, tolerances of components. In order to counteract these effects and provide an effective filter for the equipment lifetime, manufacturers generally do not design a filter tuned at the exact frequency of the harmonics that need to be mitigated.

Detuning can be expressed in the most general form as:

$$\delta = \frac{\omega - \omega_n}{\omega_n} = \frac{\Delta f}{f_n} + \frac{1}{2}\left(\frac{\Delta L}{L_n} + \frac{\Delta C}{C_n}\right) \quad (2)$$

where the subscript $n$ refers to nominal quantities and δ is referred to as detuning factor. Typical de-tuning can be between -0.02 and -0.04, and [15] calculates the optimized value as -0.0375.

Other disadvantages of passive filters include the following [5], [11], [16]:

- They can mitigate only a limited numbers of harmonics.
- The filter components are very bulky because the harmonics that need to be suppressed are usually of the low order.
- Any modifications in the grid (restructuring, adding new lines or reactive power compensation equipment etc.) can affect the effectiveness of the passive filter.
- At a specific frequency, a parallel resonance occurs between the grid impedance and the passive filter, thus leading to potential harmonic amplification. To solve such problem, the quality factor of the filter is reduced thus resulting in increased consumption of active power.

In addition to the above, the changes taking place in modern distribution systems are exposing other limitations of passive filters:

- New harmonic components have been observed on the power grid, which may be far from the filter tuning frequency, thus making the passive filter ineffective.
- With increasing harmonic levels on the system, it is likely that existing passive filters may become overloaded.

Given the above limitations, active filter applications may be more effective in some cases, and this technology will be described more in details in the next sections.

## 4.2 Active filters

The basic concept of the AF is to utilize power electronics technologies to produce specific current components that cancel harmonic currents caused by non-linear loads (such as the ones shown in Table 1). In the most common configuration, an AF consists of a voltage or current source converter, dc link storage capacitor and an output filter [5] [17].

Due to the remarkable progress in power electronics, AFs have developed significantly in the last decades, and their effectiveness relies on the following factors:

- Power circuit configurations and connections,
- Reference generation techniques,
- Filter control strategies,
- Converter types and modulation techniques,
- Rating and dynamic response of the compensated system.

Although AFs have a complex structure, require sophisticated controls topology and are costly, they achieve many benefits on power quality. In addition to harmonic compensation, they may provide compensation of reactive power, voltage imbalance and voltage fluctuation (flicker). Moreover, unlike passive filters, they do not cause harmful resonances with the power distribution system.

On the other hand, AFs have some drawbacks. An unfavourable but inseparable feature of AFs is the necessity of fast switching of high currents in the power circuit. This results in high frequency noise that may cause Electromagnetic Interference (EMI) in the power distribution systems. Therefore, there is still a need for further research and development to make this technology well-established.

Depending on circuit connections, compensation variable and configurations, AFs can be classified into four topologies:

- Series active filters
- Shunt active filter
- Hybrid active filters, composed of active and passive filter
- Combination of series and shunt AFs in a Unified Power Quality Conditioner (UPQC).

Each topology will be shortly described in the following sections.

### 4.2.1 Series active filter

The series AF, shown in Figure 12, injects a controllable current component, which is connected in series with the network through a current transformer to mitigate the voltage harmonics and maintain a sinusoidal voltage waveform [1]. It also can be applied to reactive power compensation, and to eliminate voltage sags or swells [18]. For this application, the series AF is located in close proximity to sensitive loads. If a fault occurs on nearby lines, the series AF can work as a Dynamic Voltage Restorer (DVR) to compensate the dip in the three-phase voltage and restore it to the pre-fault value [19]. The momentary amplitudes of the three injected phase voltages are controlled in such a way to eliminate any detrimental effects of a bus fault [20], [21], [22], [23]. However, Series AFs cannot be used for current imbalance compensation.

These devices are not widely used in industrial applications because they require high current ratings and increased component costs, compared to shunt filters [24].

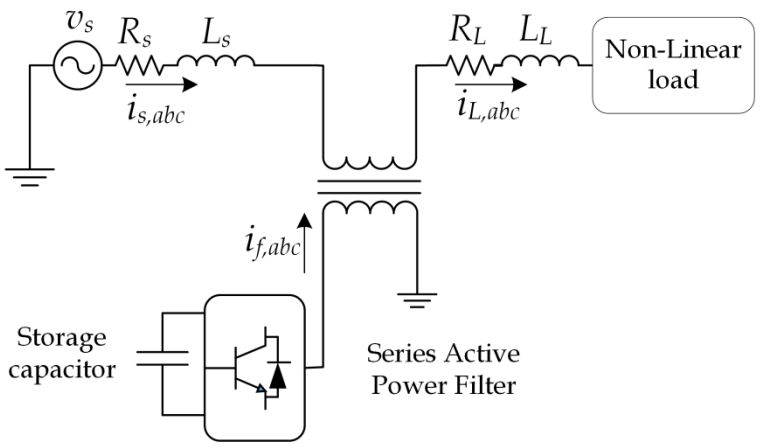


Figure 12: Series active filter connected in series between the grid Thevenin equivalent and the non-linear load.

### 4.2.2 Shunt active filter

The shunt AF is one of the most popular configurations and it is widely used for harmonic cancellation. The configuration of the shunt AF is shown in Figure 13: in this case, the shunt passive filter and the non-linear load are connected to the same bus, referred to as point-of-common coupling (PCC).

The shunt AF operates by injecting harmonic current components with the same magnitude as those introduced by the non-linear devices, but phase-shifted by 180°. As a result, the existing harmonic current components are cancelled and the source current is only the fundamental component.

The above principle is applicable to any type of loads considered as a harmonic source. Moreover, with an appropriate control scheme, the shunt AF can also compensate the device's reactive power at the PCC, thus helping to improve the power factor. As a result, the non-linear device and the shunt active filter appear to the grid as an ideal resistor/source.

The voltage source converter-based shunt AF is by far the most common type used today, due to its well-known topology and straightforward installation procedure.

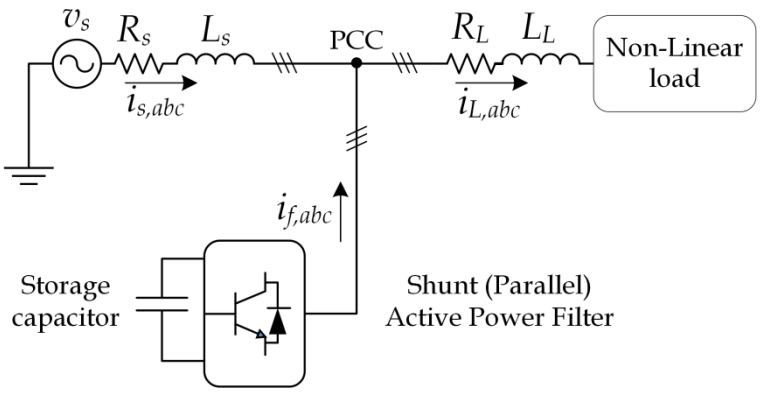


Figure 13: Shunt active filter connected at the PCC.

### 4.2.3 Hybrid active filter

Even though shunt AFs are an effective compensation system, their cost increases rapidly with increasing power capacity. As a solution, the hybrid active filters have been developed by combining active and passive filters. This configuration helps mitigating a broad range of harmonics, while maintaining a lower cost when compared to shunt AFs.

The hybrid AF can be connected to the grid in series or parallel. The hybrid AF may include a variable number of passive and active filter combinations. For example, the hybrid AF may include two passive filters tuned to the 5$^{th}$ and 7$^{th}$ harmonics, and an AF that may compensate the higher order harmonics. Figure 14 shows the configuration for a shunt connected hybrid active filter including one passive filter and one active filter [25], [26], [27], [28].

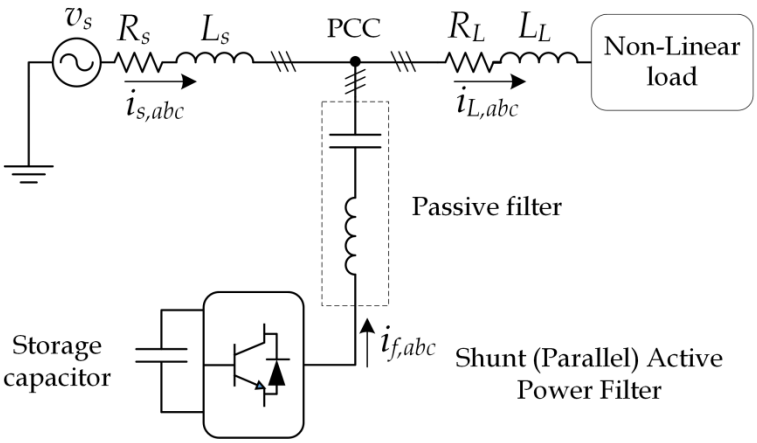


Figure 14: Shunt hybrid active filter connected to the PCC.

### 4.2.4 Unified Power Quality Conditioner

The unified power quality conditioner (UPQC) is the combination of series and shunt AFs, and employs a range of control strategies to achieve improved voltage harmonic compensation capabilities and to fully exploit the potential functionality of the two topologies, without requiring tuned passive harmonic filters. The series AF uses a direct voltage controller for voltage regulation and voltage dip compensation, together with an array of resonant harmonic controllers, to provide selective mitigation of supply voltage harmonics as seen by the load. The shunt AF regulates the dc link voltage and compensates for load unbalance and load current harmonics.

Figure 15 shows the schematic diagram of the UPQC. As a result of the operation described above, this configuration can regulate the load voltage, compensating for both source voltage dips and voltage harmonics, while simultaneously eliminating load current harmonics [29], [30]. The main drawback of the UPQC is the complexity of the control scheme [31].

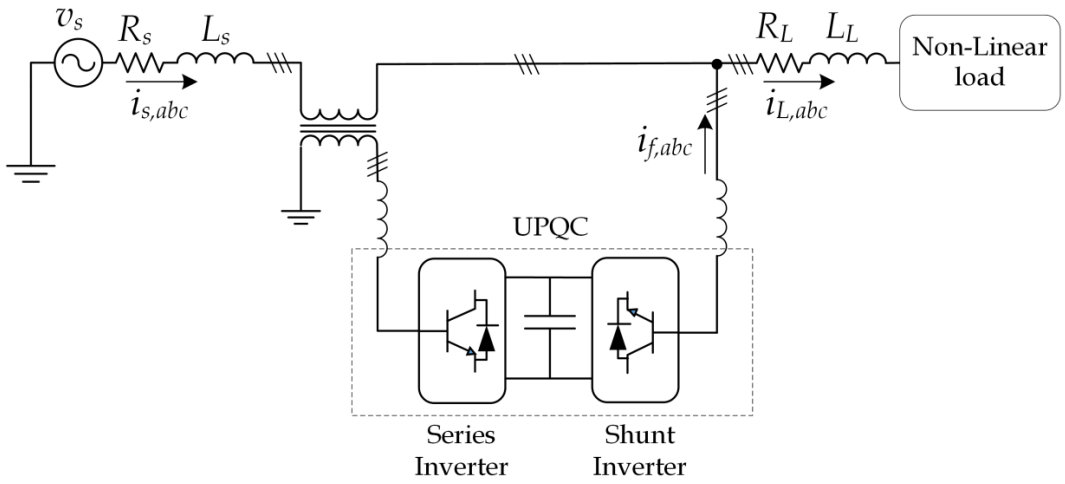


Figure 15: Three-phase configuration of the Unified Power Quality Conditioner (UPQC).

### 4.2.5 Comparison of active filters

A comparison between passive filters and the four AF topologies presented in the previous sections is provided in Table 6. In general, as the performance and control capabilities increase, the complexity and the costs also increase.

Table 5: Comparison of different filters [32].

| | Passive Filter | AFs | | Hybrid Filter | UPQC |
|---|---|---|---|---|---|
| | | Series | Shunt | | |
| Harmonic compensation | Fixed | Voltage harmonics | Current harmonics | Both | Both |
| Resonance with grid | Possible | No | No | No | No |
| Load balancing | No | No | Yes | Yes | Yes |
| Power rating | - | High | High | Small | Small |
| Number of switches | - | 6 | 6 | 4, 6 | 4, 6, 8, 12, 18, 24 |
| Total cost | Lowest | High | High | Medium | Highest |

# 5 Control schemes for active filters

The control algorithm used to regulate the AF operation can be divided into three stages:

1. Reference current generation,
2. Current loop control, and
3. Switching gate signal generation for the voltage/current source converter.

In the first stage, the reference current generation scheme extracts harmonic components from the distorted voltage/current waveforms – these components are then used as references. The second stage consists of control of the current loop, based on the reference components and the measured output filter current. The last stage is to generate the gate signals for the voltage/current source converter.

In the following sections, each one of the stages above will be explained in detail.

## 5.1 Reference current generation using harmonic extraction techniques

The first step in the design of AF control consists in generating the reference current (or, more rarely, voltage) components [12], [33]. The reference is generated from the harmonics detected in the distorted current waveforms.

Numerous extraction methods are described in literature. These methods can be implemented digitally or using analogue hardware. Figure 16 shows the classification of the extraction techniques for current/voltage reference generation in three main categories: analogue filters, traditional, and modern techniques [12], [33], [34].

Most of these approaches are implemented either in time-domain or frequency- domain. The methods implemented in time-domain include analogue filters, instantaneous $pq$ theory, synchronous rotating frame (SRF) theory, and harmonic voltage component (Vh) detection. The methods implemented in frequency-domain include Fast Fourier Transform (FFT), wavelet and dead-beat. Generally, the time-domain methods are more common and provide a faster response with a lower computational burden [12]. On the contrary, the frequency-domain methods have poor transient response, require extensive calculations, and the use of considerable memory [33], [34].

The modern techniques shown in Figure 16 are less common in the practical applications because of they require the use of advanced computation equipment [33], [34].
The following sections provide a description of the most commonly used harmonic extraction methods.

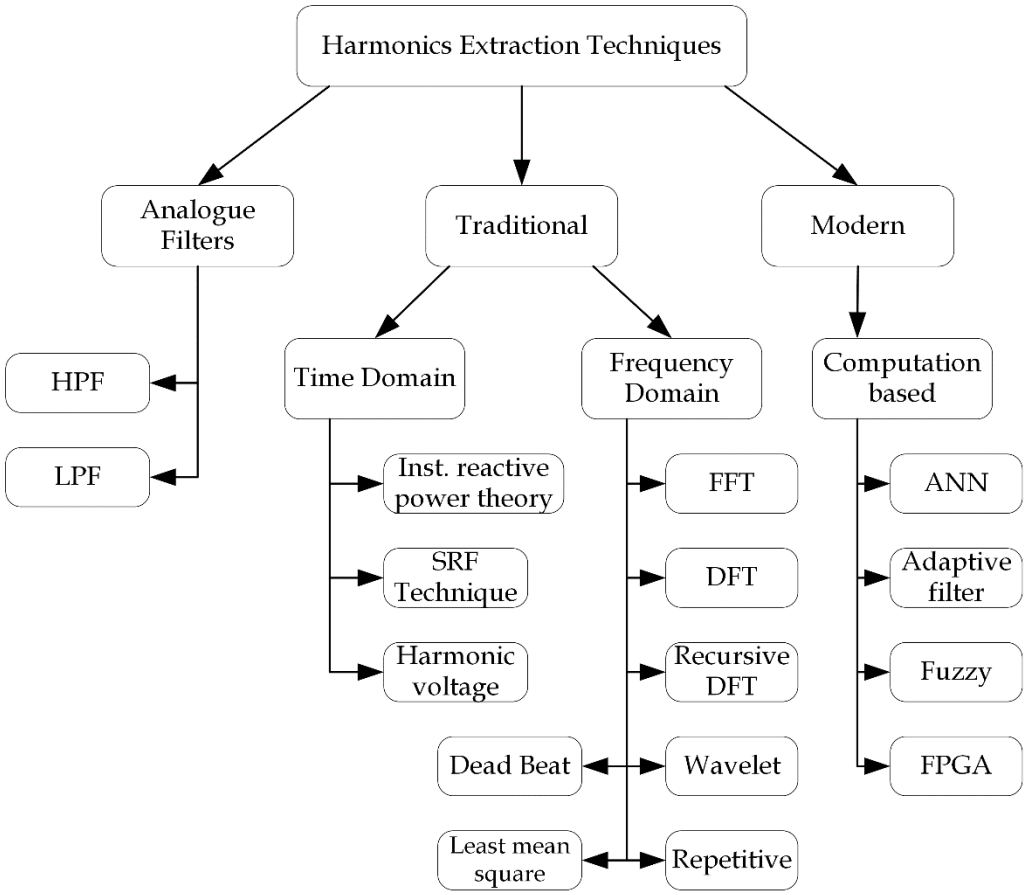


Figure 16: Classification of the most common harmonic extraction techniques [13], [33], [34]. For the acronyms list, refer to the glossary table at the beginning of the document.

### 5.1.1 Analogue Filters

#### 5.1.1.1 High-pass filter (HPF)

The high-pass filter method is straightforward and consists of removing low-order frequencies in the load current waveform. The resulting high-frequency components constitute the desired references [35].

#### 5.1.1.2 Low-pass filter (LPF)

This method is preferred over the use of high-pass filter because it reduces the effect of differentiation in the resulting filtered component. It involves isolating the fundamental component and then subtracting it from the total load current, thus yielding to the desired reference. However, this approach has some drawbacks as it suffers from magnitude and phase errors [35], [36].

### 5.1.2 Traditional methods

As mentioned earlier, these methods are differentiated into in time- and frequency-domain approaches. The most common methods are summarised in the next sections.

#### 5.1.2.1 Instantaneous reactive power theory (time-domain)

The instantaneous reactive power theory (also known as $pq$ theory), was firstly proposed in 1984 [37]. It was initially developed for three-phase systems without a neutral, and then extended for three-phase four-wire systems.

The main idea of this theory is to transform the distorted voltage/currents waveforms from three-phase $abc$ frame to stationary $\alpha\beta\gamma$ frame, by applying the Clarke transformation. The $\gamma$ component is generally set to zero and therefore is not included in the control loops. Then a set of mathematical calculations are applied to obtain the instantaneous active and reactive power components in time domain as shown in Figure 17.

This method offers a good precision and ease of implementation. However, it has some drawbacks such as slow dynamic responses, sensitive to imbalance of grid voltages, large numbers of transducers required and poor performance in case of negative and zero current compensation [38], [39], [40], [41].

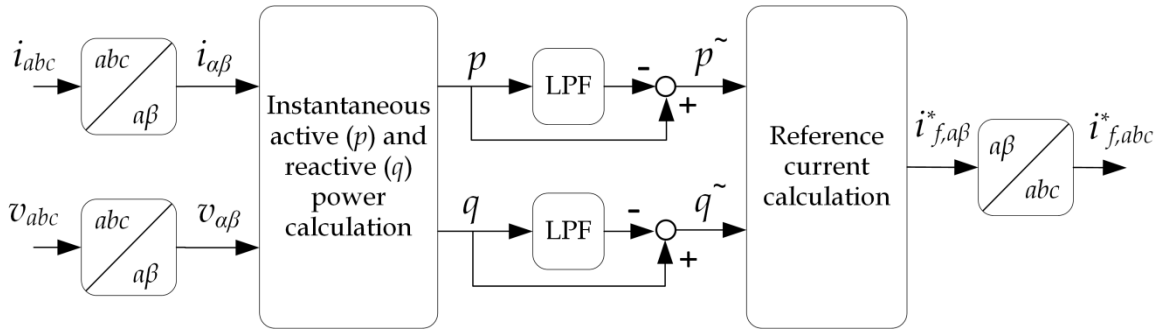


Figure 17: Instantaneous active and reactive power theory.

#### 5.1.2.2 Synchronous reference frame (SRF) theory (time-domain)

This is one of the most common approaches, also known as instantaneous $i_{dq}$ theory. Figure 18 shows the basic principle of SRF method. The first step involves transforming the load currents from three-phase $abc$ frame into a synchronous direct-quadrature ($dq0$) reference frame using the Park transformation [42]. The reference frame is synchronised with the grid voltage by using a Phase-Locked Loop (PLL). Similarly to the case described before, the $\gamma$-component set to zero and is not included in the control loops.

Then the current direct and quadrature ($d$ and $q$) components are fed to a low pass filter to separate the harmonic components from fundamental current. In the last stage, the inverse Park transformation is used to convert the instantaneous $d$ and $q$ components back into three-phase $abc$-frame components [43].

The main drawbacks of SRF theory include a requirement for large number of transducers and a delay in output responses [44].

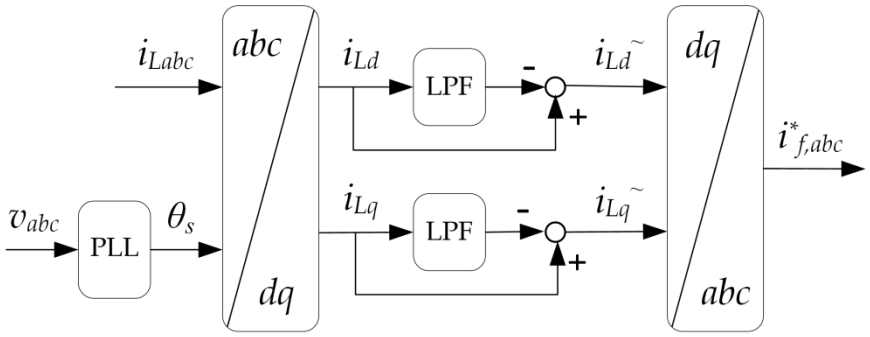


Figure 18: Principle of the synchronous reference method.

### 5.1.2.3 Harmonic voltage components (Vh) detection (time-domain)

This method requires measurement of the harmonic component of the voltage measured at the PCC. The harmonic component is then used to generate the reference current after passing it through a proportional controller.

Figure 19 shows the block diagram of the voltage harmonic detection [45]. The main drawback of this method is that harmonic voltage components are only a small fraction of the fundamental voltage components, and therefore they are difficult to measure accurately.

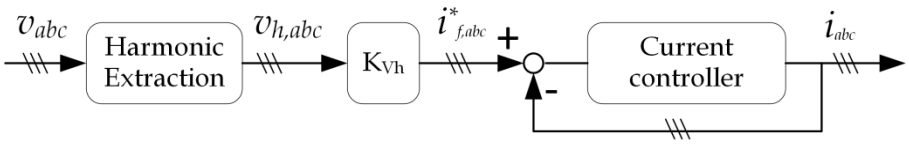


Figure 19: Reference current generation based on PCC voltage detection.

### 5.1.2.4 Fast Fourier Transform, FFT (frequency-domain)

This method is based on the application of the discrete Fourier transform (DFT) to periodic signals [46], [47], [48].

Figure 20 explains the basic concept of this method, assuming the signal under consideration is a current. The time-domain waveform is sampled with a constant frequency, thus providing the discrete samples $i_L(0) \dots i_L(n) \dots i_L(N-1)$, where $N$ is the number of samples. Therefore $n$ is an integer number between 0 and $N-1$.

The DFT of this signal is then expressed as follows [49]:

$$\boldsymbol{I}(n) = \sum_{k=0}^{N-1} i[k] e^{-j\omega kT} \tag{3}$$

where $\omega$ is the fundamental angular frequency, $T$ is the period of the original waveform and $\boldsymbol{I}(n)$ is a complex number representing each harmonic component in the frequency domain.

The DFT is characterised by a few errors, such as aliasing and leakage. However, the main drawback of this method is the computational time required, this is proportional to the square of the number of samples, $N^2$. Given that $N$ is generally at least equal to 256[3], the computational speed can be a major consideration.

However, based on the observation that the DFT includes many redundant calculations, other more efficient algorithms have been developed, including the Fast-Fourier transform (FFT). This method is based on splitting the sampled data in two datasets and applying the DFT to each one of them, thus reducing the computational speed by a factor of four. The outputs are then combined by applying some weighting coefficients, thus providing the spectral components $\boldsymbol{I}(n)$ [49].

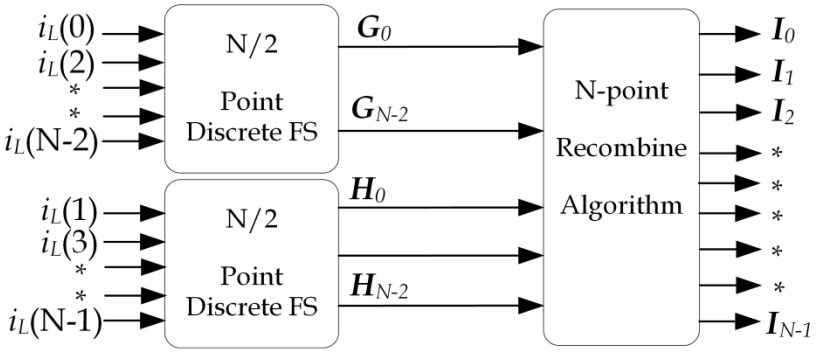


**Figure 20: Illustration of the FFT-based algorithm to extract harmonic components from a periodic current signal.**

### 5.1.2.5 Recursive discrete Fourier transform, RDFT (frequency-domain)

This method is applied to extract the fundamental current component and replaces the use of filters [28]. It provides a reference signal having an identical steady-state performance with improved computational efficiency and faster transient response, compared to traditional filtering methods [50]. RDFT technique is used to extract the real and imaginary components of the fundamental current.

Figure 21 shows the RDFT-based reference signal generator. The real and imaginary fundamental current components are extracted by the RDFT block, and then subtracted from the load current to obtain the harmonic-only components [50]. The filter reference currents are obtained by adding the load *d* and *q* current components and the dc-link reference current to the harmonic components.

The drawback of this approach is that it does not provide correct output under unbalanced operating conditions. A solution to this issue is explained in [51], where positive sequence components are extracted using Fortescue decomposition to obtain active and reactive current components under both balanced and unbalanced load conditions.

[3] N is the length of the transform and it is required to be a power of 2 for the DFT. In order to have a reasonable approximation of the spectrum, in general N>256 is adopted. Given that the DFT requires $N^2$ complex multiplications, the computational effort increases significantly with the accuracy. For N=256. The DFT requires 65536 complex multiplications. This result is reduced to 1024 when the FFT is applied, thus leading to a 98% reduction in the calculations [137].

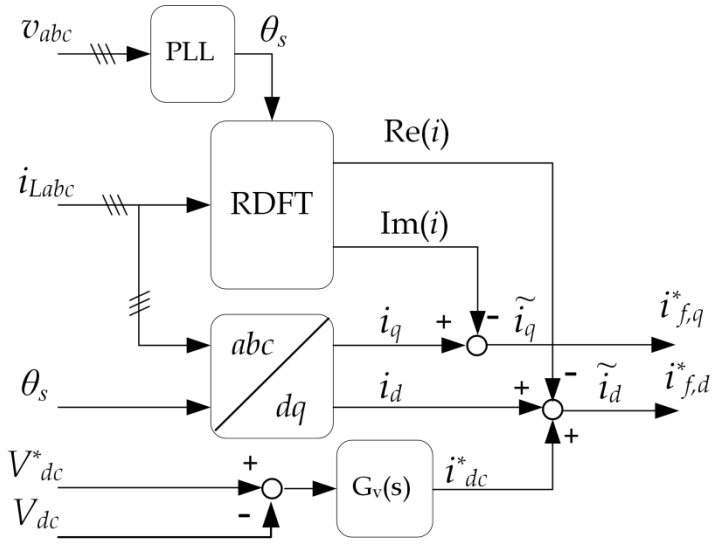


Figure 21: The RDFT based reference current generation.

#### 5.1.2.6 Wavelet transform (WT)

One of the limitations of processing techniques based on the Fourier transform is that the resulting signal loses information about the time associated to each frequency signal. In order to overcome this limitations, the basic functions of wavelet transforms are waves localized in time- and frequency-domains.

Wavelet analysis is a powerful signal-processing tool that is particularly useful for the analysis of non-stationary signals. Wavelets are short-duration time-varying waveforms with zero mean and fast decay to zero amplitude at both ends, which are dilated and shifted to vary their time-frequency resolution.

In wavelet analysis, the wavelet function is compared to a section of the signal under study, obtaining a set of coefficients that represent how closely the wavelet function correlates with the signal in that section. More details about this technique can be found in [52], [53], [54].

### 5.1.3 Modern extraction methods

Recently, the fast development in processors and microprocessors opened new doors for the development of new computer-based extraction techniques. Most of these techniques are represented in frequency-domain and include notch filter and adaptive notch filter (ANF) [55], adaptive neural network [56] [57], fuzzy least mean square (LMS) [58], least mean square algorithm [59], deadbeat controller [60], energy shaping repetitive control [61], synchronized filtered-x (SFX) control [62], , delta-sigma modulation [63], and field-programmable gate array FPGA implementation [64], etc.

The main disadvantages of these methods include: poor transient response extensive calculations time, the use of considerable memory, and a delay in the extraction of harmonics which can be at least one period.

## 5.2 Current loop control

The next step after generating the reference current is to choose a suitable control strategy for the active filter. Based on the location where the load current is measured, the current control loops can be divided into two categories:
- Direct current measurement.
- Indirect current measurement.

The direct current measurement is shown in Figure 22. In this case, the load current and the AF currents are measured and fed to the controls. The operating principle is then as follows: the harmonic current components are extracted from the load current, and the AF generates harmonic currents with the same magnitude but opposite in phase, to achieve harmonic cancellation at the PCC.

When using this method, there is no need to measure the source current. All errors such as the parameter's uncertainty, the measurement delays, or control errors will appear in the grid current as unfiltered harmonic content. The main advantage of this method is in terms of stability.

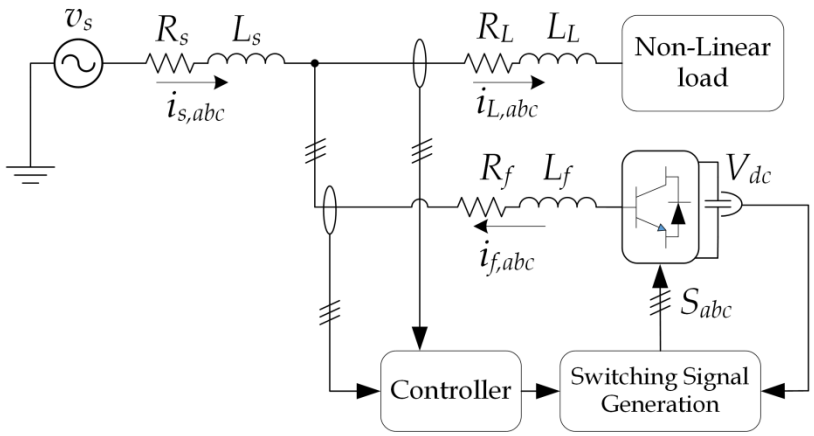


Figure 22: Schematic diagram of direct current measurement scheme.

Figure 23 shows the diagram of the indirect current measurement method. In this case, the source current and the load current are measured. The control system reference in this case is the sinusoidal current component at fundamental frequency extracted from the grid current.

For either one of the approaches presented in Figure 22 and Figure 23, different control strategies can be applied. The control unit plays the most important role in AF performance because it generates the required reference quantities used to generate the switching signals.

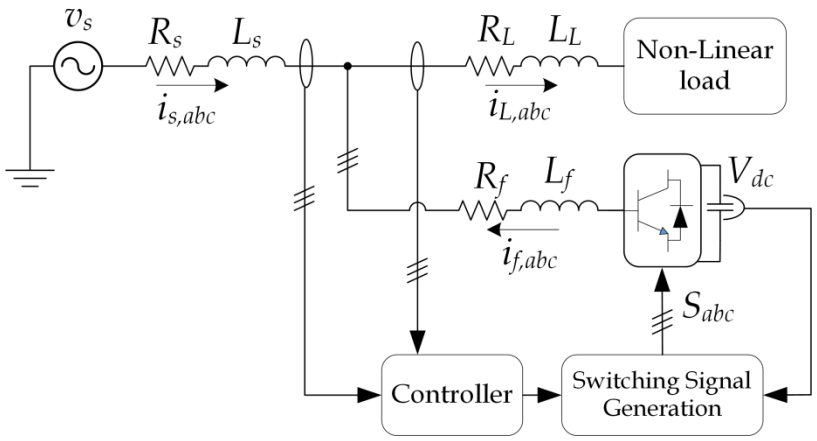


Figure 23: Schematic diagram of indirect current measurement.

The most common control strategies used for AF operation will be presented in the next sections. Each method can be applied to either the direct or the indirect control scheme.

### 5.2.1 Control method based on instantaneous power

This method is based on the power theory proposed in [37], and it is illustrated in Figure 24. It calculates active and reactive power based on direct and quadrature current components obtained in the SRF as described in Section 5.1.2.2:

$$\begin{bmatrix} p_L \\ q_L \end{bmatrix} = \begin{bmatrix} v_d & v_q \\ -v_d & v_q \end{bmatrix} \begin{bmatrix} i_d \\ i_q \end{bmatrix} \tag{4}$$

where $p_L$ is the load active power and $q_L$ is the load reactive power. Each power component is composed of two terms:

$$\begin{aligned} p_L &= P_L + \tilde{p}_L \\ q_L &= Q_L + \tilde{Q}_L \end{aligned} \tag{5}$$

The first term represents a constant component, while the second is a time-varying component due to harmonics at various frequencies. In the direct control method both $p_L$ and $q_L$ are used to generate the reference current, while in the indirect control method only $p_L$ is used, as shown in Figure 24. In the direct control method, to obtain unity power factory, the reactive power reference must be zero.

By using a low pass filter with appropriate cut-off frequency, the time-varying components can be cancelled, thus obtaining a constant value for the load power$P_L$. The reference active power is then calculated as the sum of the dc link power $P_{dc}^*$ and the load power $P_L$, as shown in Figure 24.

This method allows the compensation of both harmonic currents and reactive power at the same time, it offers a good precision and it is easy to implement. However, it has some drawbacks such as delay in output responses, sensitive to imbalance of grid voltages, large numbers of transducers required and poor performance in case of negative and zero current compensation [38], [39], [40].

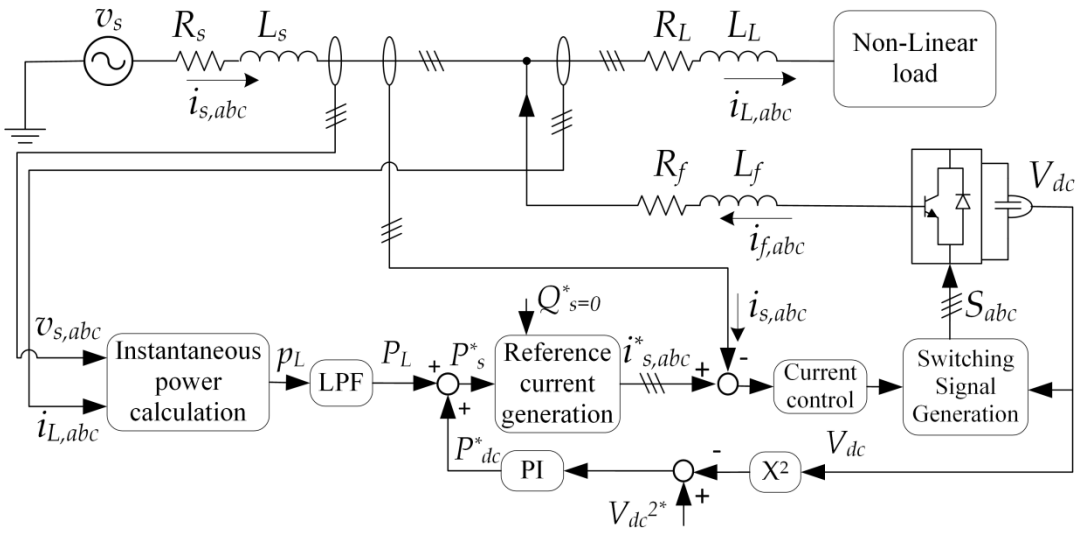


Figure 24: Indirect control based on instantaneous power (PQ) theory.

### 5.2.2 Control based on instantaneous currents

The main principle of this method is very similar to the one described in Section 5.2.1, with the difference that it is based on the direct reference currents calculation rather than power calculation. The schematic diagram of the indirect control method based on instantaneous currents is shown in Figure 25.

Using the load currents and the voltage angular position generated by a PLL circuit, the load direct current component $i_{Ld}$ is calculated. Similar to the power terms described in Section 5.2.1, this current is expressed as the sum of two components:

$$i_{Ld} = I_{Ld} + \tilde{\imath}_{Ld} \tag{6}$$

where $I_{Ld}$ is a direct component and $\tilde{\imath}_{Ld}$ is a time-varying component due to harmonics. By using a low pass filter with appropriate cut-off frequency, the dc component can be extracted, which represents the fundamental grid current.

The source reference current $i_s^*$ is then generated from the sum of the fundamental grid current components and the current produce from the dc voltage controller:

$$i_s^* = i_{L,d}^* + i_{dc}^* \tag{7}$$

In this method the value of reactive current $i_q$ is generally set to zero, thus allowing compensation of current harmonics and reactive power at the same time.

The reference current is transformed in the $abc$ frame and compared to the measured source current $i_{s,abc}$. The error signal $i_{s,err}$ is then fed to the current controller and the output is the reference voltage used for switching signal generation.

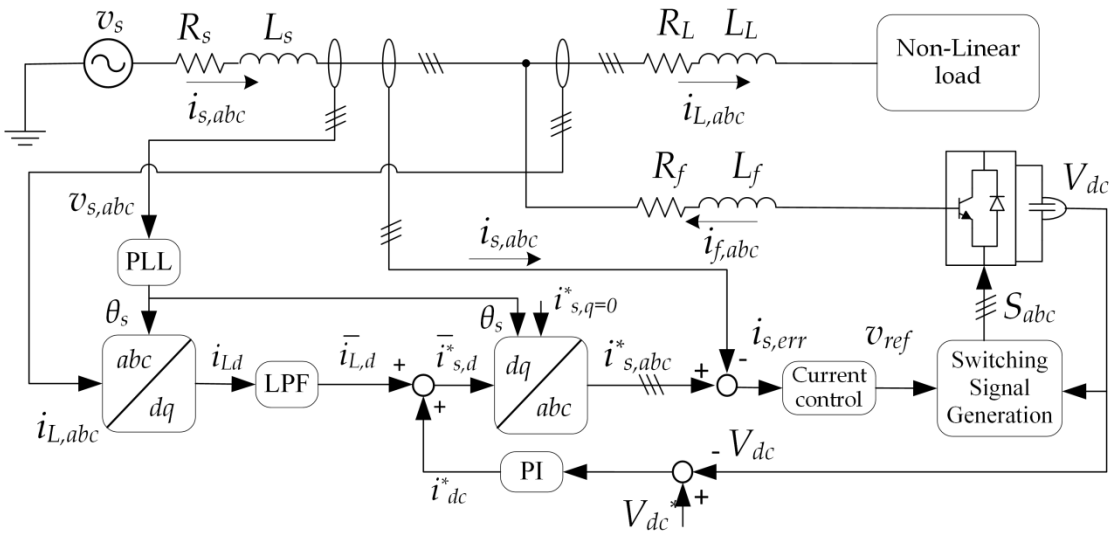


Figure 25: Indirect control method based on the instantaneous currents.

### 5.2.3 Control method based on synchronous reference frame

This method is one of the most popular control schemes for balanced systems, and its structure is shown in Figure 26. This technique is similar to the one presented in the previous section with three main differences:

- both direct and quadrature currents are used ($i_{Ld}$ and $i_{Lq}$)
- the time-varying current components are extracted from $i_{Ld}$ and $i_{Lq}$ (while in the previous method the constant component was extracted).
- the current control is carried out in the SRF, with two closed-loop current controllers. The closed loop controllers are usually conventional proportional integrator (PI) regulators, due to their low steady-state error and fast dynamic response.

As shown in Figure 26, the load currents are transformed from $abc$ frame into $dq$ reference frame using Park transformation [42]. The current in $dq$ reference frame contains a direct and a time-varying harmonic component (at multiple frequencies), as discussed in the previous section. A low pass filter is used to extract the time-varying current components and use them as reference quantity.

These reference quantities are then compared with the actual filter output current and the resulting error signals are fed into the PI controller. Since the aim of the controller is to maintain the steady state error to zero a feedforward term is used to calculate the filter reference voltages $v^*_{fd}$ and $v^*_{fq}$.

If the three-phase system is unbalanced, negative-sequence $d$ and $q$ components will be generated. In this case, applying the conventional PI controller to the direct value in the $dq$ frame won't achieve the required performance. Hence, a double synchronous reference frame for positive and negative sequence components is an option, as discussed in the next section.

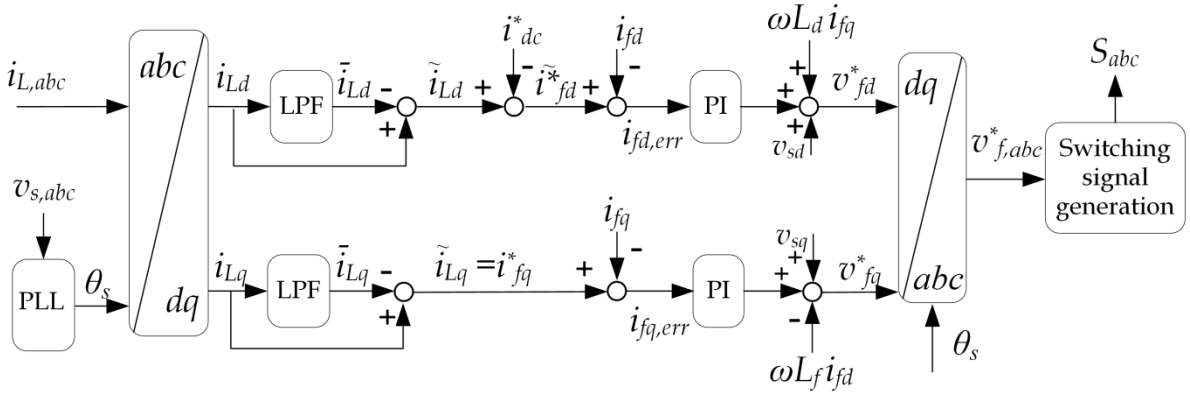


Figure 26: Direct control of AF based on synchronous reference frame.

### 5.2.4 Control method based on double synchronous rotating reference frame

A more accurate approach to control current or voltage under unbalance conditions consists of employing two synchronous reference frames, 'double synchronous reference frame' (DSRF) controllers [65], [66]. Both SRFs rotate at the fundamental frequency but in opposite direction. They therefore provide a solution to control both positive- and negative-sequence current components, individually and simultaneously.

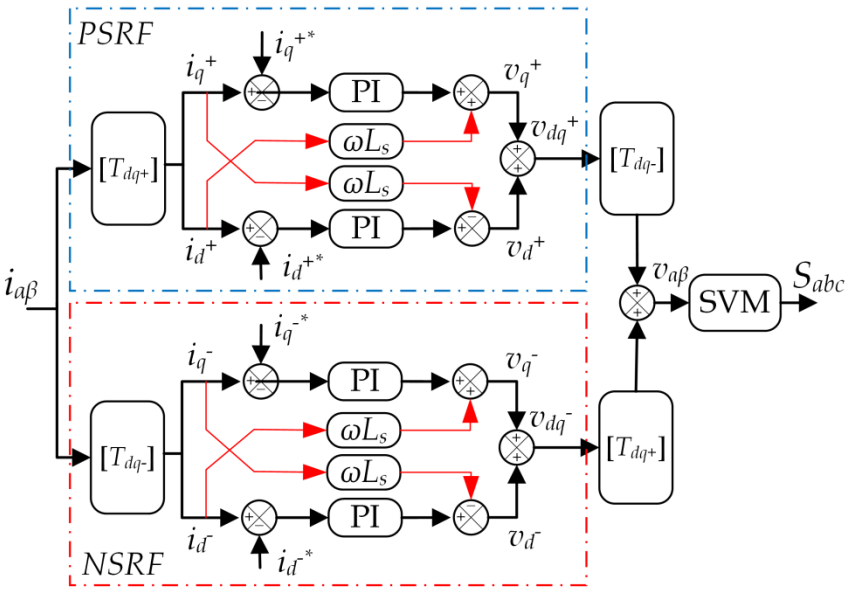


Figure 27: Double synchronous reference frame controllers: PSRF is the positive-sequence SRF; NSRF is the negative-sequence reference frame.

DSRF strategy is widely employed for PLL and grid voltage synchronisation under unbalanced conditions [66]. It includes a pair of PI controllers in both PSRF and NSRF, as shown in Figure 27.

For most standard DSRF control strategies, the measured unbalanced three-phase currents are transformed into positive and negative rotating SRFs using Park transformation [37]:

$$i_{dq}^{+} = i_{dq+}^{+} + i_{dq-}^{-} e^{-j\,2\omega_s t}, \quad \begin{bmatrix} i_d^{+} \\ i_q^{+} \end{bmatrix} = \underbrace{\begin{bmatrix} i_{d+}^{+} \\ i_{q+}^{+} \end{bmatrix}}_{DC\ terms} + \underbrace{\begin{bmatrix} i_{d-}^{-}\cos(2\theta_s^{+}) + i_{q-}^{-}\sin(2\theta_s^{+}) \\ -i_{d-}^{-}\sin(2\theta_s^{+}) + i_{q-}^{-}\cos(2\theta_s^{+}) \end{bmatrix}}_{AC\ terms} \tag{8}$$

$$i_{dq}^{-} = i_{dq-}^{-} + i_{dq+}^{+} e^{j\,2\omega_s t}, \quad \begin{bmatrix} i_d^{-} \\ i_q^{-} \end{bmatrix} = \underbrace{\begin{bmatrix} i_{d-}^{-} \\ i_{q-}^{-} \end{bmatrix}}_{DC\ terms} + \underbrace{\begin{bmatrix} i_{d+}^{+}\cos(2\theta_s^{-}) + i_{q+}^{+}\sin(2\theta_s^{-}) \\ -i_{d+}^{+}\sin(2\theta_s^{-}) + i_{q+}^{+}\cos(2\theta_s^{-}) \end{bmatrix}}_{AC\ terms} \tag{9}$$

where $\theta_s^{+} = \omega_s t$ and $\theta_s^{-} = -\omega_s t$.

The currents in the positive and negative SRFs are not pure $dc$ components due to the cross-coupling effect between the two SRFs, thus generating oscillatory terms with twice the fundamental frequency $2\omega_s$ overlapped with the dc quantities [67]. The amplitude of the oscillations in one of the SRFs matches the $dc$ amplitude of the other and vice versa. These oscillations will then appear in the resulting error signals at the input of the PI controllers, thus resulting in steady-state errors and increased current fluctuation.

To achieve full control of the injected currents under unbalanced conditions, the oscillations with frequency $2\omega_s$ must be cancelled out. Several solutions oriented to overcome this issue have been presented, such as decoupled DSRF controller [67] [68], adaptive notch filter [65] [69], and sequence components extraction method [70].

Although no reference could be found describing the application of the DSRF to AF control, this method has been included in the literature review because it appears more robust than the conventional SRF control. Therefore, it will be considered as one option in the development of AF control to be carried out in WP2.

### 5.2.5 Dc-link capacitor voltage regulation

The dc-link capacitor voltage regulation algorithm involves estimating the amount of dc-link charging current $i_{dc}$ needed by the AF to constantly maintain the dc-link voltage $V_{dc}$ at a desired level $V_{dc}^{*}$ .

This algorithm continuously compares the measured $V_{dc}$ with the reference value and minimizes the resulted error by using a PI regulator [71], [72] via a voltage control loop, as shown in Figure 28.

When the error between the measured $V_{dc}$ and the predetermined set-point value is minimized, the maximum effective magnitude of $I^*_{dc,max}$ will be generated. Subsequently, by utilising the phase synchronization angle $\theta_s$, $I^*_{dc,max}$ will provide three-phase reference currents in-phase with the grid voltage [45], [73]:

$$i^*_{sa} = I^*_{dc,max} \sin(\theta_s) \tag{10}$$

$$i^*_{sb} = I^*_{dc,max} \sin\left(\theta_s - \frac{2\pi}{3}\right) \tag{11}$$

$$i^*_{sb} = I^*_{dc,max} \sin\left(\theta_s + \frac{2\pi}{3}\right) \tag{12}$$

where the angle $\theta_s$ is the angular position generated using a PLL circuit.

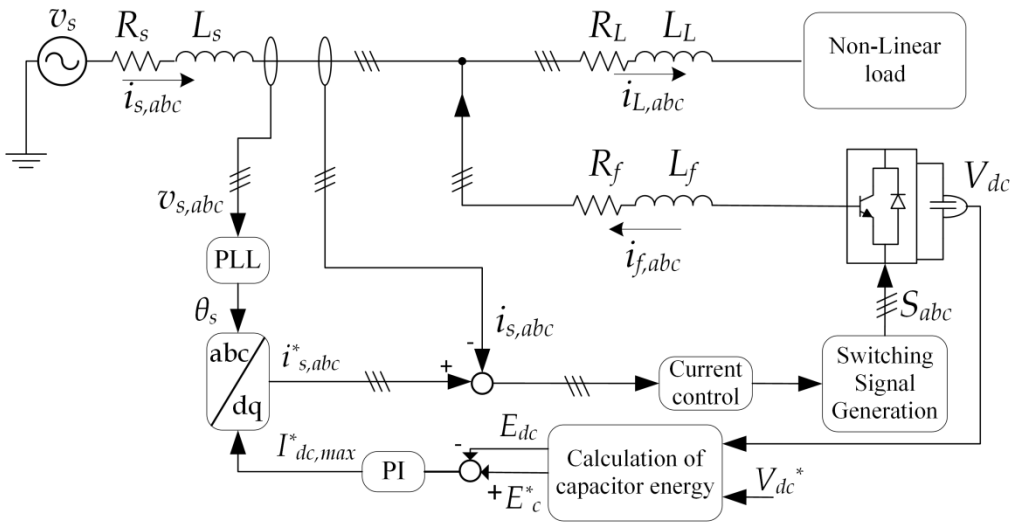


Figure 28: Indirect control method using dc voltage regulation.

### 5.2.6 Other control methods

In addition to the strategies discussed in the previous sections, the literature describes other algorithms to control AFs. These strategies are rarely used in the practice, however, for completeness, they are listed below, together with some of the main references:

- dead-beat controller [60], [74], [75];
- repetitive control [61], [74], [76];
- one-cycle control [74];
- linear control technique [74], [77];
- sliding mode control [74], [78];
- ramp comparison current control [74];
- predictive control [74], [79];
- fuzzy control [74], [80];
- artificial neural network [81], [82], [83];
- particle swarm optimization [74];
- reduced dc link voltage [84], [85];
- negative sequence current control [74], [86];
- other optimisation techniques [87], [88].

Two comparison studies between numbers of techniques for different AF configurations are described in [74], [89].

## 5.3 Converter types and gate signal generation techniques

After generating the reference current components and selecting a suitable control method, the output of the controller represents the reference signal used to compensate the selected harmonics. The compensating currents are injected by using a power converter.

Two main types of converters are used for the deployment of AF: current-source converter and voltage-source converter. A comparison between the two topologies is provided in Table 6 [90]. In addition to these two main configurations, more recently several papers have described the use of multi-level converter topologies [90], [91], [92].

Table 6: Comparison between current-source and voltage-source converters

| Comparison criteria | Current-source converter | Voltage-source converter |
|---|---|---|
| No of Phases | Usually three-phase | Single-phase and three-phase |
| Function of Particular Filter | Injects current at PCC to eliminate current harmonics of nonlinear load | Acts with Superimposed current control loop to compensate current harmonic |
| Power Rating | Medium power | Low or Medium power |
| Control | Complex | Simple |
| Speed of Response | Medium Response | Fast Response |
| Switching Frequency | Around 2-5 kHz | Around 20-30 kHz |
| dc Energy Storage | Large dc Inductor | Large dc Capacitor |
| Control Method | PWM of dc-link current | PWM of dc-link voltage |
| Converter circuit | Figure 29 (a) | Figure 29 (b) |

The current-source converter, with an inductor on the dc side, is shown in Figure 29 (a). This device needs a complex control strategy, so it is not commonly used in low power applications. However, it is more convenient for medium and high power applications, where several current-source converters are connected in parallel [31], [41] thus providing high current-carrying capability.

The voltage-source converter has a large capacitor connected to the dc voltage bus, as shown in Figure 29 (b). This converter is more common for low- and medium-power AF applications due to its low weight, low cost, simpler control strategy. This topology can be developed for multi-level versions to boost the performance with lower switching frequencies [24], [31], [93].

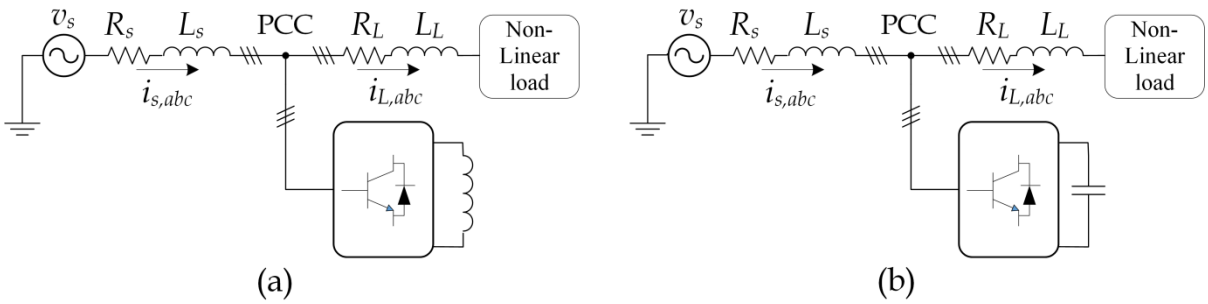


Figure 29: Converter types (a) current-source and (b) voltage-source.

The next section presents a discussion of the most common techniques used to generate the switching signal for the converter in AF control.

### 5.3.1 Pulse width modulation

Pulse-width modulation (PWM) is a popular signal-generation technique, based on modulating the power converter with a fixed-frequency. The most commonly used PWM techniques are carrier-based, and they are known as sinusoidal PWM (SPWM), triangulation, sub-harmonic, or sub-oscillation techniques [17], [94].

Figure 30 (a) shows the principle of the SPWM technique: the measured current is compared to the reference current, and an error term is fed to a controller, that generally is based on the use of a PI regulator [17]. The output of the controller is a reference voltage that is compared with a triangular carrier signal. The frequency of the carrier corresponds to the converter switching frequency and it is in the order of few kHz. The output of this comparison provides the switching signals $S_i$ and $\bar{S}_i$ to the converter [94]. Figure 30(b) shows more in detail how the switching signals are generated. The same procedure is repeated for all three phases.

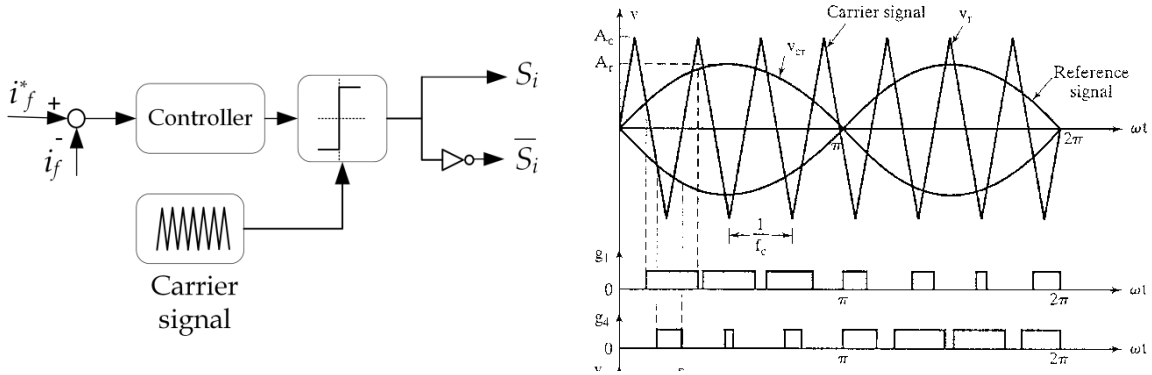


(a) (b)

Figure 30: Pulse width modulation techniques. (a) Controller and carrier signal. (b) Switching signal generation [94].

In the SPWM technique, the modulation index is defined as follows:

$$M = \frac{\hat{V}_c}{V_r} \tag{13}$$

where $\hat{V}_c$ and $\hat{V}_r$ are the peak modulating and carrier signal voltages, respectively. The modulation index is generally maintained between 0 and 1 to provide a linear relation between the reference signal and the output. The relationship between the phase voltage, the line voltage and the dc link voltage are as follows:

$$V_{phase} = \frac{1}{2\sqrt{2}} M \cdot V_{dc} \tag{14}$$

$$V_{line} = \frac{\sqrt{3}}{2\sqrt{2}} M \cdot V_{dc} \tag{15}$$

When $M = 1$, the maximum peak value of the fundamental phase voltage is $V_{dc}/2$, the maximum phase-to-phase (line) output voltage is 61.2% of the dc-link voltage in the linear modulation range.

When the neutral point on the ac side is not connected to the dc side midpoint, the phase currents will depend only on the voltage difference between phases. An additional zero-sequence signal (ZSS) can be added as shown in Figure 31: this allows increasing the modulation index M and reducing the harmonics generated by the power converter [95].

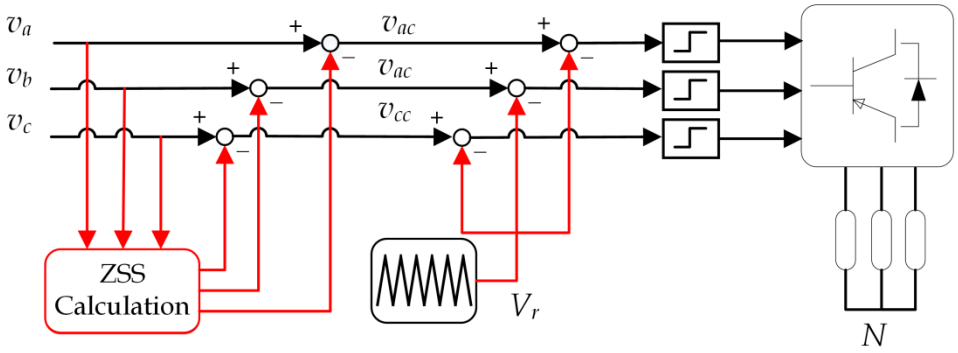


Figure 31. A schematic diagram of the modulator with the additional ZSS.

Due to its versatility, several alternative PWM methods have been developed. These techniques are divided into continuous and discontinuous. In the continuous PWM techniques, the modulation waveform is always within the triangular peak boundaries, and the carrier waveform and the modulating waveform intersect in every carrier cycle. In the discontinuous pulse-width modulation (DPWM) techniques, the modulation waveform has a segment, which is clamped to the positive or negative dc -link voltage. In these segments, some power converter switches do not switch. Therefore, reduced switching losses (on average 33%) can be achieved [95].

**Error! Reference source not found.** shows the most commonly used carrier waveforms used f or PWM. Only phase a reference waveform is shown for readability. The first row shows continuous modulation techniques, while the second row discontinuous modulation techniques. (a) is the same waveform shown in Figure 30 and is reported for completeness; (b) shows the third harmonic injection pulse width modulation (THIPWM); (c) shows the space vector pulse-width modulation (SVPWM); (d)-(e) show three different types of DPWM waveforms. The SVPWM technique will be described more in details in the next section.

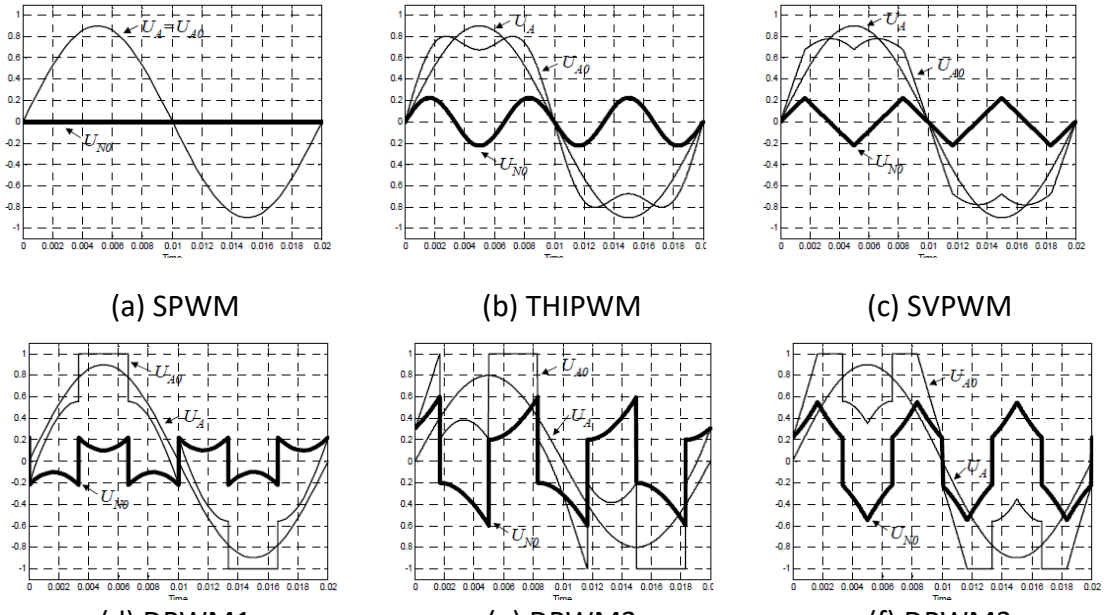


Figure 32: PWM techniques based on different carrier signals [95].

SPWM is a popular technique because it presents several advantages: it easy to implement, it is characterized by a fixed switching frequency and by a low harmonic content. As a result, the switching losses are low [97], in particular when compared to hysteresis control (described in Section 5.3.3).

The main drawback of SPWM is that it cannot generate a high output voltage, since the maximum phase-to-phase (line) output voltage is 61.2% of the -link voltage in the linear modulation range.

### 5.3.2 Space vector pulse width modulation

Space vector PWM (SVPWM) technique (also referred to as space vector modulation, SVM) is widely employed for three-phase voltage-source and current-source converters-based AF.

The zeros, non-zero, and reference voltage vectors are shown in Figure 33. The eight vectors correspond to the operating state of the power converter. The active six vectors ($V_1$ - $V_6$) divide the space plan into six equal area (six sectors) displaced by $60^0$, which can be represented by a complex vector expression as:

$$V_i = \begin{cases} \frac{2}{3} V_{DC} \exp^{j(i-1)\pi/3} & ; \quad i = 1,2,...6 \\ 0 & ; \quad i = 0,7 \end{cases} \tag{16}$$

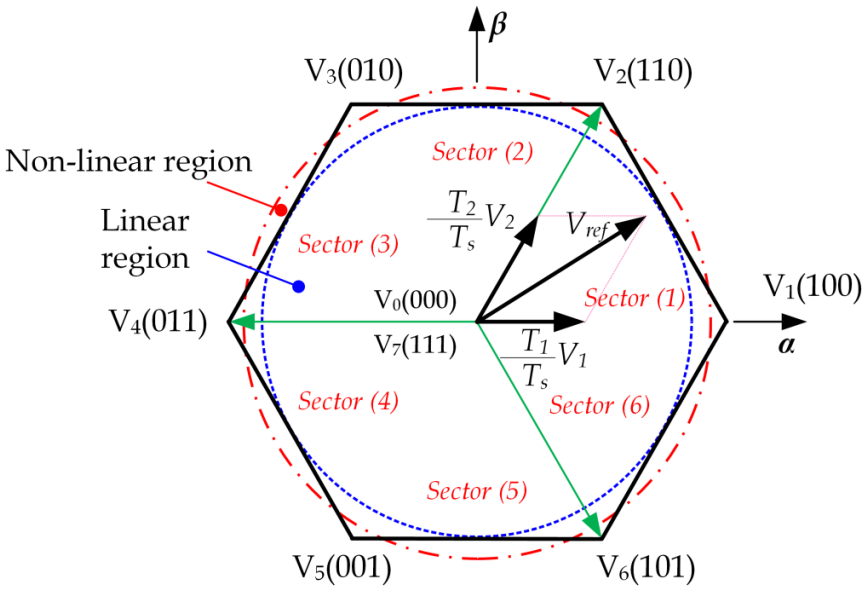


Figure 33: Space voltage vectors and sectors used for SVM.

Furthermore, in Figure 33, the linear and non-linear operating regions are identified. For the linear operation region, $V_{ref}$ remains within the hexagon, which means that the maximum amplitude voltage is equal $V_{dc}/\sqrt{3}$ and the modulation index $M$ is equal to:

$$M = \frac{V_{dc}/\sqrt{3}}{2V_{dc}/\pi} = 0.9068 \quad (17)$$

The value of the instantaneous reference voltage $V_{ref}$ is used to predict the operating sector. For instance, if $V_{ref}$ is located in Sector 1, it can be obtained by employing the two nearest active voltage vectors $v_1$and $v_2$ along with the zero vector $v_0$:

$$T_s V_{ref} = t_1 v_1 + t_2 v_2 + t_0 v_0 \quad (18)$$

where $t_1$ and $t_2$ are the time spent on the output voltage vectors $v_1$and $v_2$ respectively and $t_0$ is the time spent on the zero vector$v_0$, and $T_s = 1/f_s$ is the sampling time. The following relationship should be always verified:

$$t_1 + t_2 + t_0 = T_s \quad (19)$$

The process described above is shown graphically in Figure 34 [96].

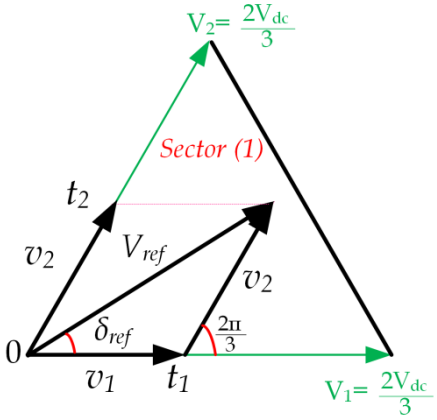


**Figure 34: Example of calculation of a voltage vector located in *Sector 1.* $V_{ref}$ is obtained as the combinat $v_1, v_2$ *and* $v_0$ .**

Operating in the nonlinear region (also called over-modulation region) is used to increase the range of maximum output voltage up to 100%. This technique has been widely discussed in literature [96] , [97].

Recently, SVM has become the most common PWM technique for digital implementation due to the following advantages [98]:

- Compared with the conventional sinusoidal PWM, SVM can increase the maximum output voltage with maximum line voltage approaching to 70.7% of the dc -link voltage (compared to SPWM's 61.2%) in the linear modulation range.
- Therefore, this method yields a higher efficiency, a better voltage total harmonic distortion (THD), and, for machine applications, a higher torque with a higher speed range [99], [100].

The main disadvantage of this technique is that it requires accurate selection of the correct operating vectors and the calculation of the duration times to achieve satisfying results. Therefore, it is more complex to implement than other methods.

### 5.3.3 Hysteresis control techniques

The hysteresis current control methods is a well-known approach to control the current and generate the switching gate signals for the voltage/ current converter.

The main concept behind this technique is to keep both the control references and tracking variables within a setting hysteresis band. For current control, a two-level hysteresis comparator is used as seen in Figure 35 (b). As long as the error is within the positive and negative hysteresis band, no switching action is taken. Switching occurs whenever the error exceeds the tolerance band as shown in Figure 35 (b) [101].

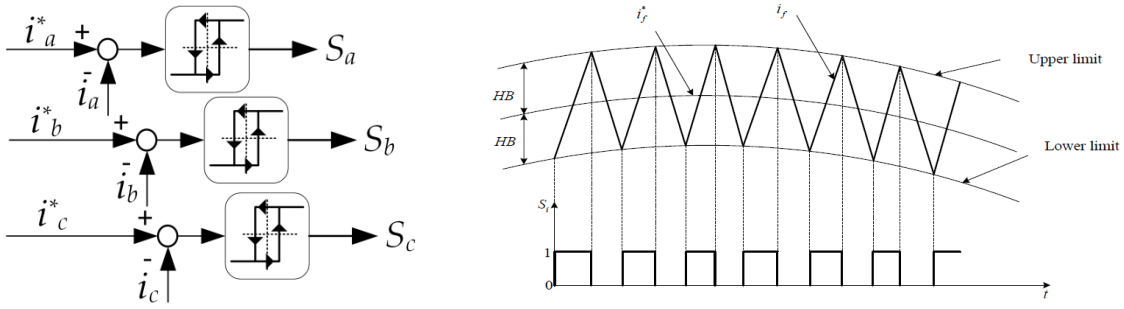


(a) (b)

Figure 35: Hysteresis controller technique. (a) Tracking reference and switching signal. (b) Hysteresis comparers.

The hysteresis current control is the fastest gate signal generating method with minimum hardware and software requirement. The main advantages of this approach are: simplicity, extreme robustness, good stability, fast dynamic and automatic current limiting characteristics. The main drawback consists in the uneven switching frequency, resulting in widely spread switching harmonics, which are difficult to filter out and may possibly stimulate the resonance between the active filter and the power grid [102]. The irregular switching also affects the converter efficiency and reliability, involving overrating of the switches [74], [103].

To mitigate the inherent drawback of hysteresis controller, new hysteresis control strategies such as “modulated hysteresis control” [104] and “variable hysteresis band” [105] have been proposed.

# 6 Active filter applications based on power rating

Examples of active filters applications based on power ratings will be illustrated in this section, divided in low-power applications, medium-power applications, and high-power applications.

The power rating and the speed of response play a major role in deciding the control philosophy to implement, among the ones presented in Section 5.

## 6.1 Low-power applications

Low power applications (<100 kvar) are associated with hospitals, residential areas, commercial buildings, and a wide range of small to medium-sized factory loads and motor-drive systems.

This range of applications employs AFs with high-pulse-number PWM voltage- or current-source converters. Their response time is much faster than other techniques, ranging from 10 µs to 10 ms. This type composes of the following two categories: single-phase systems and three-phase systems.

Figure 36 shows a low power AF designed and manufactured by NANCAL. This unit is compact and can be easily fitted within a residential or commercial building.

Several other manufacturers provide AFs for low power applications: examples of such devices, together with their ratings, include: SIEMENS 4RF1010-3PB0, 380–480 V; SCHNEIDER AccuSine PCS+, 380-690 V; DELTA ELECTRONICS, INC APF2000, 200–480 V; DELTA power quality correction (PQC) Series AF, 432-880 V.


Figure 36: Wall mounted low power AF used in hospital manufactured by NANCAL [106].

### 6.1.1 Single-phase systems

Single-phase active filters [107] are generally available with low power ratings and they are suitable for applications in commercial or educational buildings with computer loads, or in small factories, where the current harmonics can be dealt with in proximity to the load. Thus, several lower-power filters can be connected on a given distribution site rather than using one large filter on the incoming supply. This allows for more selective compensation when the operating conditions vary.

The main advantage of single-phase filters is that they are rated for low power and hence can be operated at relatively higher frequencies leading to improved performance.

### 6.1.2 Three-phase systems

For three-phase applications, the choice of filter/configurations depends on whether the three-phase loads are balanced or not. At relatively low power levels (<100 kVA), a three-phase system can use either three single-phase or one three-phase compensator.

For balanced loads, a single three-phase-power converter configuration is employed [1], [108], [109]. This is acceptable if there is no requirement to balance currents or voltages in each phase and the aim is simply to eliminate as many current harmonics as possible, assuming that the magnitudes and respective phase angles in each phase are the same.

For unbalanced load, currents or unsymmetrical supply voltages, especially in three-phase four-wire distribution systems, three single-phase power converter circuits [110] or alternative configurations such as the ones described in [24] are preferred solutions. The connection of three single-phase filters is recommended by some designers [1], [110] especially those who do not rely upon standard power converter configurations such as lattice structures, switched capacitor techniques and power-regulator configuration.

## 6.2 Medium-power applications

This category includes three-phase systems ranging from 100 kVA to 10 MVA [1], [111]. Medium- to high-voltage distribution systems and high-power high-voltage drive systems, where the effect of phase unbalance is negligible, fall within this classification.

Figure 37 shows an example of AF used in the medium range of power. At these voltage levels, generally only three-phase AFs are implemented. Given that higher power rating are involved, the switching frequency is slower. The speed of response in this range is of the order of tens of milliseconds.

Using AFs with a single level converter at medium power applications is challenging, therefore, research is focused on increasing the power rating of the AFs by using a multilevel converter [112], [113], and Hybrid AFs [114].

Figure 37: Front and rear view of AF designed by NANCAL, 3-phase, 400 V, 740 A [106].

## 6.3 High-power applications

The implementation of high-power active filters (>10 MVA) is extremely cost ineffective, because the lack of high switching frequency power devices that can control the current flow at such power ratings is a major limitation [115]. Voltages of a few hundred kilovolts cannot be tolerated even by state-of-the-art semiconductor devices (which can withstand only a few kilovolts). The series-parallel combinations of these switches is possible, but difficult to implement and cost-ineffective.

However, harmonic pollution at the transmission system level, is much lower than in distribution systems. In the practice, the effect of harmonics at these voltage levels are minimised with the installation of several medium- and low-power AFs downstream. The required response time for such cases is in the range of 10 s, which allows an effective protection coordination with other devices installed on the system, [5].

One of the few applications of active filters in high-power systems is the Japanese bullet train (Sinkansen) [1], which uses a parallel combination of several active filters. The control and co-ordination requirements of these filters are, however, quite complex [1].

Table 7 summarises AF applications based on power rating and the other features described in this section.

Table 7: AF classification according to the rated power [34].

| | Low power | | | Medium power | High power |
|---|---|---|---|---|---|
| | 1 -phase | 3-phase | | | |
| | | 3*1 phase | 3 phase | | |
| **Power ratings** | <100 kVA | | | 100 kVA to 10 MVA | >10 MVA |
| **Response time** | 10 µs | 100 µs to 10 ms | 1 ms to 10 ms | 100 ms to 1 s | about 10 s |
| **Control techniques** | Simple | | | Less complex | Complex |
| **Switching frequency** | High | | | Medium | Low |
| **Size** | Small | | | Medium to large | Large |
| **Cost** | Low | | | Medium to high | High |
| **Application** | Residential areas, small factory loads, motor drive systems, distribution systems, commercial buildings | | | High power and high voltage drive systems | Power transmission grids, ultra-high power dc drives, and dc transmission systems |

## 6.4 Cost of harmonic mitigation

The cost of harmonic mitigation solutions varies broadly and depends on numerous factors, including: the harmonic frequencies to compensate, the system voltage level and short circuit level, ingress protection (IP) of insulation class rating, quality factor for the inductors (in the case of passive filters) and speed of response (in the case of active filters) [108], [116], [117], [118], [119], [120].

In order to provide an estimate of the costs, various sources have been used, from manufacturers (Schneider Electric, ABB, Eaton, TC and GE), to literature sources.

The results of the literature search are summarised in Figure 38, where the cost of each solution is shown as a function of the kvar rating. In this figure, all solutions proposed are at the low voltage level, since this is the most common application for active filters, as explained in Section 6.1. As expected, the costs for active filters are larger than the costs of passive filter, and this explains the most common use of passive filters.

However, the increased sophistication of Active Filter controls and the possibility to embed active filter operation within other power converters makes this solution more attractive and is the basis for the proposed project, as it will be discussed in the next section.

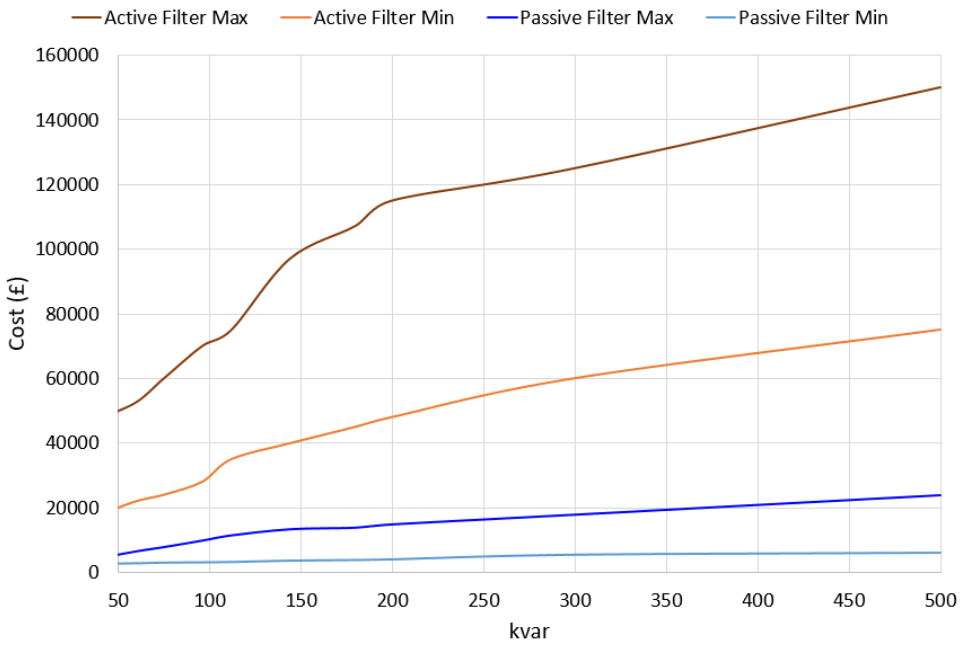


Figure 38: Summary of costs for passive filters and active filters solutions, based on the rating.

# 7 Active filter as an ancillary service

Ancillary services are advanced control functionalities necessary to support the transmission of electric power from the power producers to the customers [121]. They refer to a variety of functions or operations beyond generation and transmission that are required to maintain grid stability, safety, reliability and security [122].

According to the 2017 UK ancillary services report, they are divided into four groups: energy balancing (reserve) services, margin (system security) services, voltage regulating services, and whole system control services [121]. The most commonly deployed ancillary service are:

- Black start
- Voltage control and support
- Frequency regulation
- Reactive power compensation
- Load following
- Spinning Reserve
- Harmonic Compensation (or active filtering)
- Network Stability

More details about each one of the services above can be found in [121] and [122].

The power converters used in distributed wind generation or PV farms have a potential to provide several ancillary services, such as reactive power compensation, voltage regulation, flicker control and harmonic compensation [123], [37], [124], [125], [126].

Due to solar irradiance variation during the day, PV inverters have an operation margin, in terms of current, which can be used for current harmonics compensation. This possibility is known as ‘multifunctional operation’ [124], and is illustrated in Figure 39. Figure 39(a) shows an ideal operating condition where the PV inverter supplies the rated power thorough the day, while Figure 39(b) shows the measured operation curve of a PV inverter. In this case, power generation covers approximately 30% of the total operation area. The remaining area (approximately 70% as shown in Figure 39(c)) can be used to provide ancillary services [127].

A similar situation may occur during times of peak generation and low demand: under these conditions, the output power of the PV inverters may be curtailed, thus releasing further capacity to provide ancillary services [2], [124].

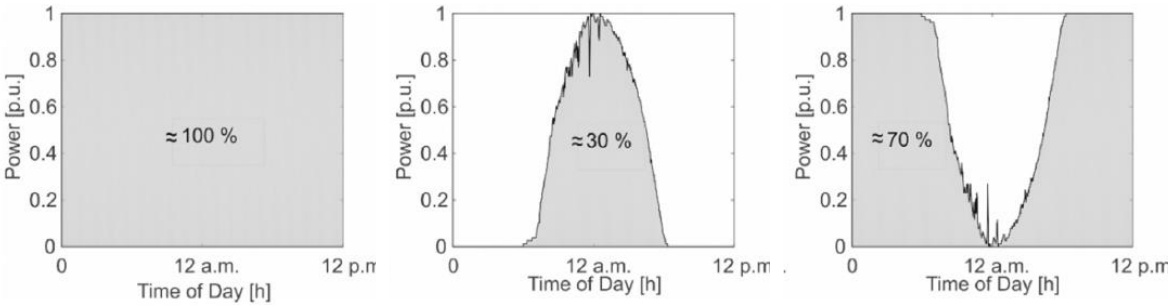


(a) (b) (c)

**Figure 39: Operation curve of a PV inverter during under different conditions. (a) Ideal operating condition; (b) Operation curve of a real PV plant during a measurement day. (c) Available operation area for ancillary services [127].**

## 7.1 Previous approaches to combined power control and harmonic mitigation[4]

The use of PV inverters to compensate harmonic currents generated by non-linear loads has been proposed already in the literature [2], [124], [125], [128]. In these works, harmonic compensation is provided as ancillary service in parallel with active power injection. A similar concept has been proposed for other power-converter based devices, such as full-inverter or partial-inverter wind power generation [3], [4] [129], and STATCOMs [130].
Different control approaches are available to perform this functionality, but the principle is the same, in spite of the device under consideration and of the control strategy: when active filtering is provided as ancillary service, the reference waveform fed to the current regulator includes two components: fundamental reference current and harmonic reference current.

The fundamental reference current is generally obtained by the active or reactive power signal. The harmonic reference current can be calculated by applying any of the control schemes described in Section 5. As a result, numerous schemes can be designed, as shown in [2], [3], [4], [113], [124], [125], [127] - [131], [132], [133] [134]

The next sections will describe three different schemes to exemplify the above described functionality.

### 7.1.1 Example 1: Control based on alpha beta and harmonic extraction based on LPF

Figure 40 shows the diagram of the multifunctional PV inverter proposed in [124] In principle, this diagram is very similar to the ones shown in Figure 22 and Figure 23: the main difference is that the active filter is replaced by the combination of a PV panel and the corresponding PV inverter. In this case, the PV inverter current $i_{f,abc}$ and the source current $i_{s,abc}$ are monitored, and the load current $i_{L,abc}$ and is obtained as the sum of the two.

[4] In some of the subsections the notation may be different from the rest of the literature review because figures extracted from the referred publications have been used. When possible, the notation has been harmonised.

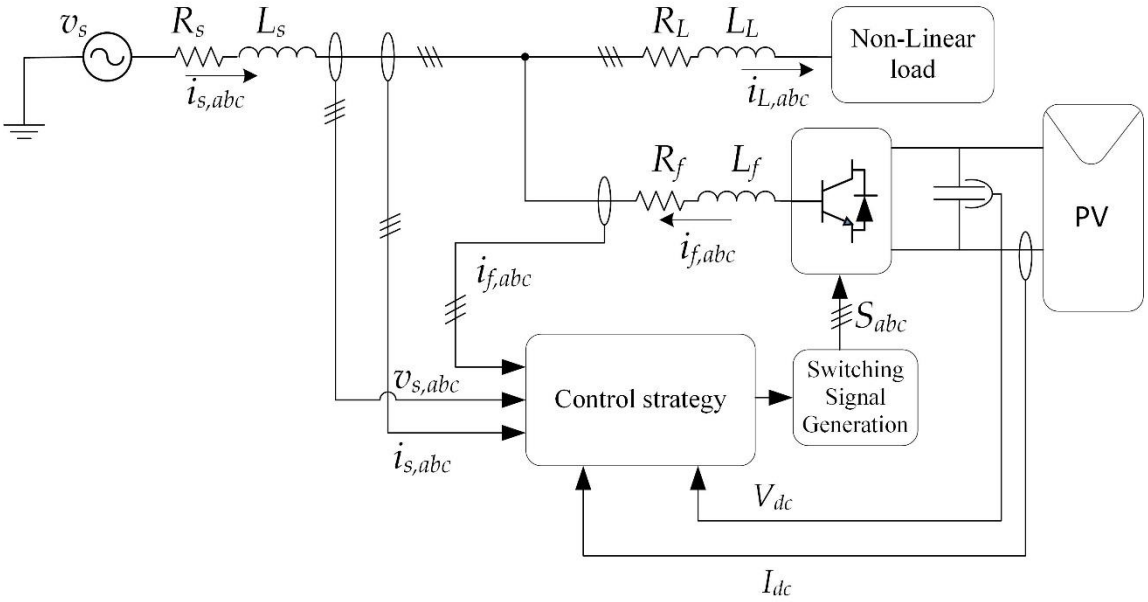


Figure 40: Grid-connected photovoltaic system based on three-phase multifunctional inverter [124] .

An overview of the control strategy for this system is illustrated in Figure 41: a maximum power point tracker algorithm (MPPT) is used to generate the reference dc-bus voltage. Comparing the reference dc voltage with the actual dc voltage of the PV system and using the PI controller, the reference active power $P^*$ is generated, representing the output of the real power from the PV system as seen in Figure 41. The reactive power reference ($Q^*$) is set to zero for unity power factor in this case, but other values could be used.

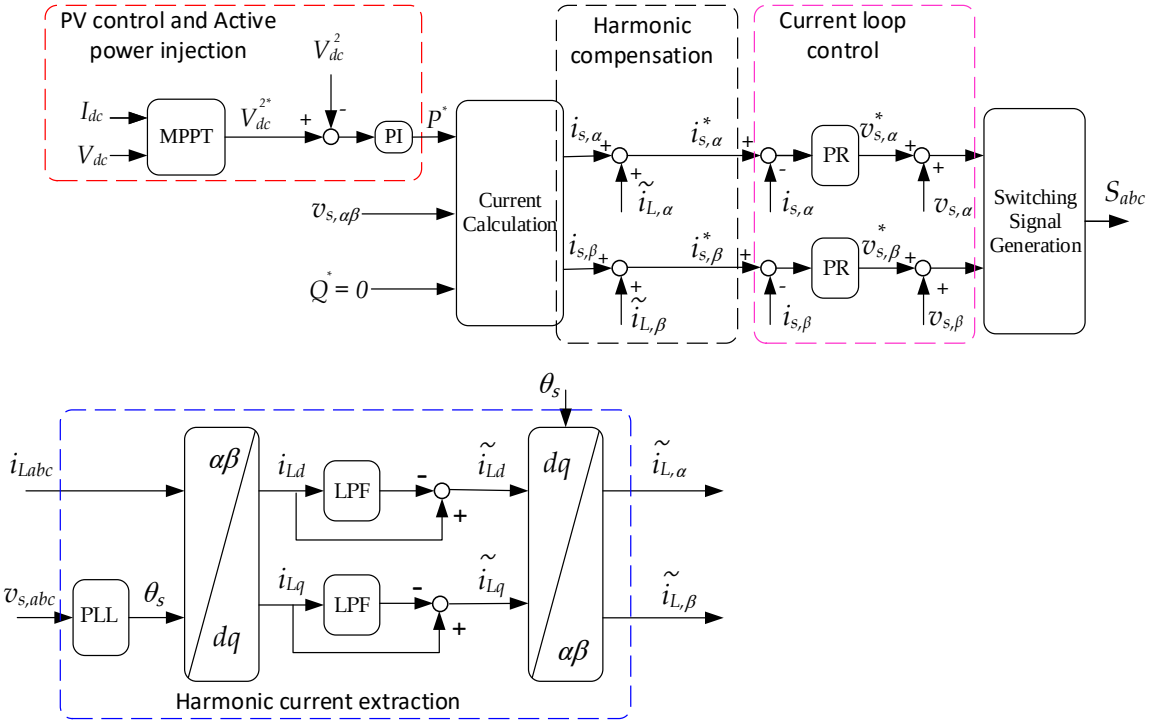


Figure 41: Control algorithm of the multifunctional PV inverter with harmonic current injection proposed in [124]

The current calculation block includes a 'harmonic saturation' algorithm that allows the calculation a derating coefficient $k$, with $0 \leq k \leq 1$. This coefficient is introduced to express curtailment of the harmonic currents injected by the PV inverter and it is required to reduce the harmonic-mitigation contribution of the PV inverter at times when all (or almost all) of its apparent-power rating is required for real-power export.

The calculation of this coefficient is shown in Figure 42. A peak detection algorithm is used to obtain the maximum value of phase $a$ current reference, formed by the sum of the average and oscillating current component. This maximum value is compared with the inverter current limit. An anti-windup PI controller generates the derating coefficient $k$. This coefficient is then applied to scale the harmonic currents. An alternative formulation of the derating coefficient is described in [135].

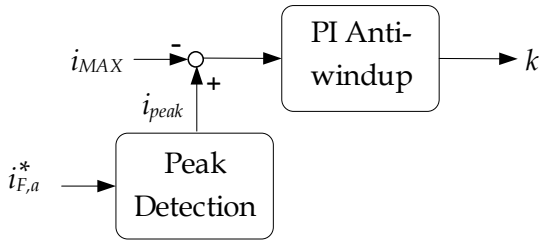


Figure 42: Harmonic saturation scheme for harmonic current proposed in [124].

The inverter reference currents are then obtained as the sum of fundamental current components $i_{s\alpha\beta}$ and the oscillating components $i^{\sim}_{L\alpha\beta}$:

$$i^*_{s,\alpha\beta} = i_{s,\alpha\beta} + i^{\sim}_{L,\alpha\beta} \tag{20}$$

Since the control variables are represented in $\alpha\beta\gamma$ frame, a proportional resonant (PR) controller is required to track the reference currents.

### 7.1.2 Example 2: Control based on SRF and harmonic extraction based on LPF

The control algorithm proposed in [131] studies a system similar to the one shown in Figure 40. The main difference between the control proposed in [131] and the one described in [125] consists in the use of the $dq0$ transformation. Other papers, such as [125], present a control strategy based on the same approach.

The current regulator for this method is shown in Figure 43. The inner current control loop is implemented in the SRF frame presented in Section 5.2.3.

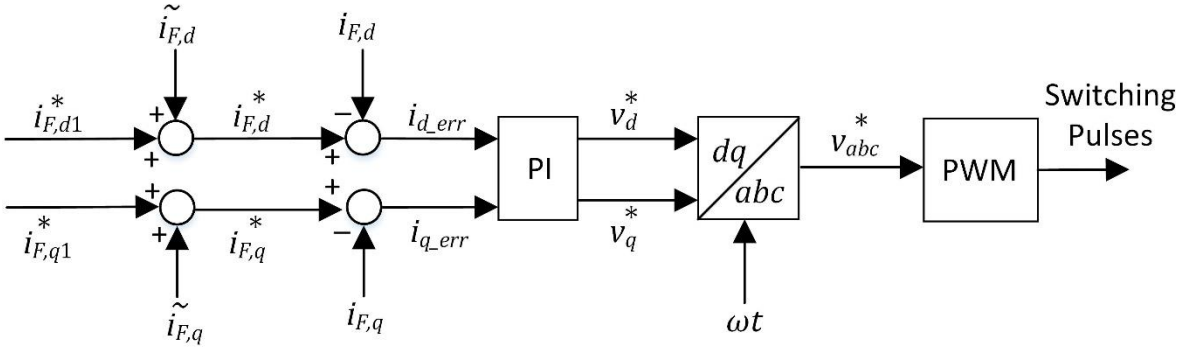


Figure 43: Fundamental and harmonic current controller based on synchronous reference frame [131].

The fundamental reference current components $i^*_{F,d1}$ and $i^*_{F,q1}$ are obtained from irradiance and power factor setting at the PV terminals. The harmonic reference current components $i^{\sim}_{F,d}$ and $i^{\sim}_{F,q}$ are obtained from the current measurement at the non-linear load terminals Figure 44. The current harmonics are extracted from the load current using the SRF method described in Section 5.1.2.2. The load currents in the $dq$ domain ($i_{L,d}$ and $i_{L,q}$) are filtered to remove the average component. This component corresponds to the fundamental current in the three phase ($abc$) domain. In this method, the derating coefficient is used as in [124] to limit the amplitude of the reference currents.

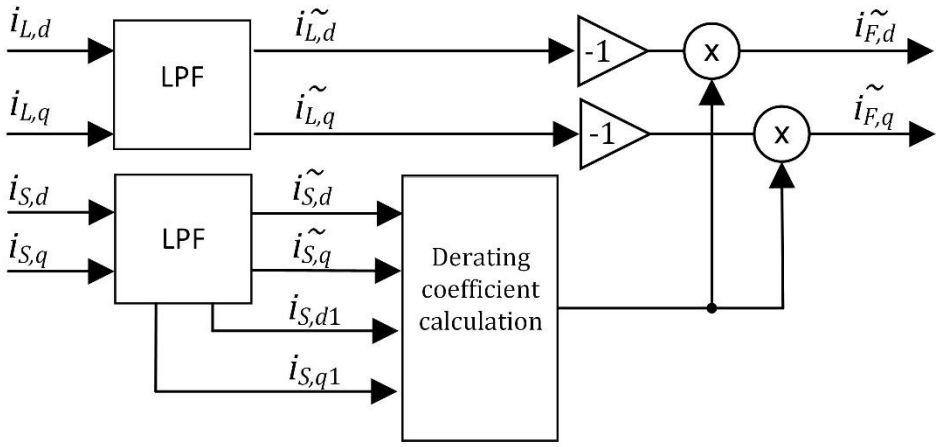


Figure 44: Reference harmonic currents calculation [131].

### 7.1.3 Example 3: Predictive control for modular multilevel cascaded converters

In [113], a new application of modular multilevel cascaded converters (MMCC) for combined active harmonic current elimination and reactive power compensation is presented. This work is included in this literature review to show that other power-electronics based devices, in addition to PV inverters, can be used to provide AF operation as an ancillary service.

The method described [113] is based on simultaneously extracting harmonic components and reactive element in the load current. A predictive control algorithm is employed for inner current loop control [73], and a LP filter in the SRF frame for current harmonics extraction. Figure 45 shows the overall block diagram of the control scheme for the MMCC system, which is divided into four main parts: submodule (SM) capacitor voltage balancing control, MMCC reference current generation, modified predictive current control, and a multilevel pulse width modulation scheme. In this case, similarly to the works presented in the previous sections, a LP filter is deployed to extract the harmonic current components.

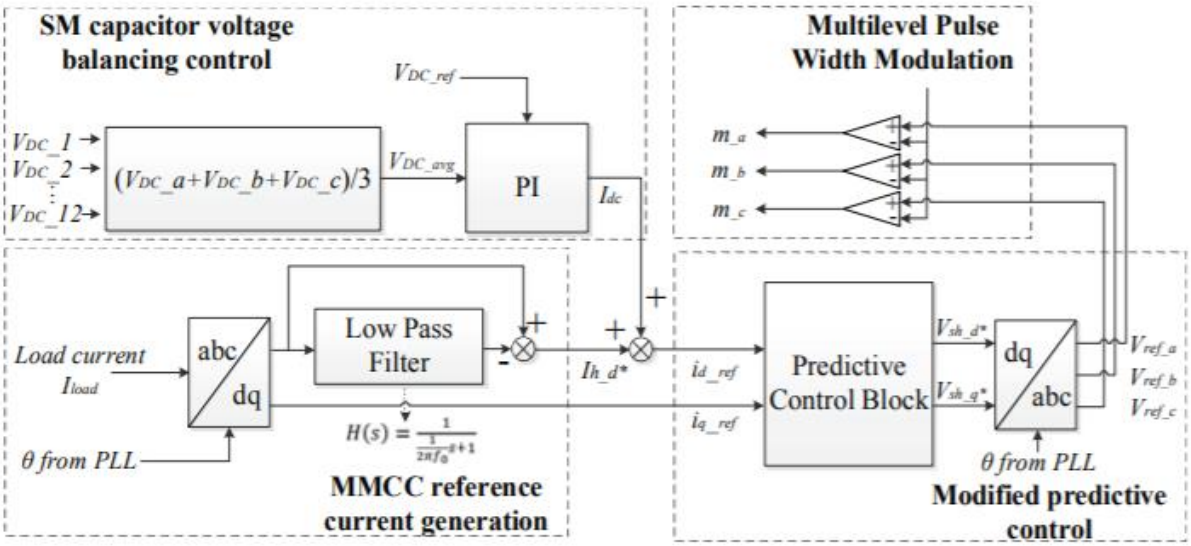


Figure 45: Block diagram of the control algorithm described in [113].

## 7.2 Previous combined AF simulation results

In this section, simulation results will be presented from the papers outlined previously to demonstrate the performance of power converters used to provide AF operation as ancillary service.

### 7.2.1 Simulation results for Example 1

Figure 46 shows the current waveforms for Example 1 [124] , referring to the single-line diagram shown in Figure 40. The first waveform shows the source current (labeled as $I_G$), the second figure shows the PV inverter current (labeled $I_s$) and the third figure shows the load current (labeled $I_L$). The source rated voltage is 13.8 kV, while the PV inverter rated voltage is 220 V.

At the beginning of the simulation, the grid current is severely distorted, while the PV inverter current is sinusoidal – indicating that the PV inverter is injecting only fundamental power. At $t$ =2 s, current compensation is enabled. As a result, the source current harmonic content decreases, while the PV inverter output current shows a visible distortion. It is important to make two observations on this waveform:
- the PV inverter current appears to have a different harmonic content from the grid current because the fundamental current amplitude of the two waveforms is different.
- the harmonic currents injected by the inverter are opposite in phase to the harmonic currents injected by the grid – this can be noticed by observing the different shape of the harmonic current peaks. Harmonic compensation does not affect visibly the distortion in the load current.

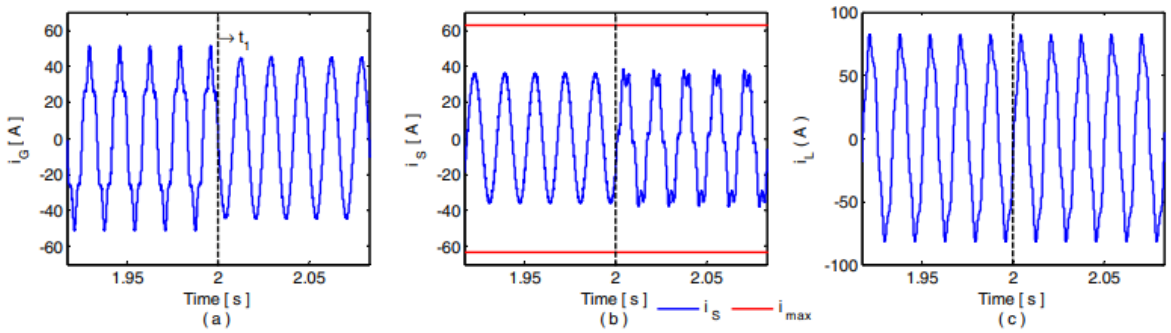


Figure 46: Current waveforms for the method presented in [125] during harmonic compensation, grid current $I_g$, inverter current $I_s$, load current $I_L$ [127].

The simulation results shown in Figure 46 indicate that PV inverters can be effectively controlled to provide harmonic current compensation while injecting fundamental power.

### 7.2.2 Simulation results for Example 2

The system studied in [131] is similar to the one shown in Figure 40: a non-linear load and a PV inverter are connected to the same PCC, and then a single-feeder connects the PCC to the rest of the grid. The high side of the PV inverter transformer is rated 33 kV, while the secondary side is rated 350 V.

Figure 47 illustrates a case when no AF operation is implemented. The first waveforms shows phase A current at the primary side of the transformer (the PV inverter output), while the second graph shows phase A current measured at the source (referred to as 'feeder current' in this work). For $t$ < 0.4 s, the inverter operates close to full power and the non-linear load is not connected. Both PV inverter output current and the source current are sinusoidal. At $t$ = 0.4 s, the non-linear load is connected, and this causes distortion in the feeder current, while the PV current remains sinusoidal, since harmonic compensation is not activated. At $t$ = 0.5 s, the utility request curtailment of the inverter power output; as a result, the transformer current and the feeder current amplitude decrease, with harmonic content unchanged.

Figure 48 shows the same simulation with harmonic compensation implemented. A third graph is added to illustrate the variation of the coefficient $k$. For $t$ < 0.4 s, the inverter operates at full power and the load is not connected. The coefficient $k$ is equal to zero because the inverter operates close to full rating. At $t$ = 0.4 s, the non-linear load is connected, and the feeder current is distorted. Since the coefficient $k$ is equal to zero, the inverter does not generate harmonic currents. At $t$=0.5 s, the utility request curtailment of the inverter power output; once the power has been sufficiently reduced, at $t$=0.68 s, the coefficient $k$ starts increasing to unity. As a result, inverter is allowed to inject harmonic currents, the transformer primary current is distorted and the level of harmonics in the feeder current decreases. The reduction is more evident when the feeder current is compared to the waveform shown in Figure 47.

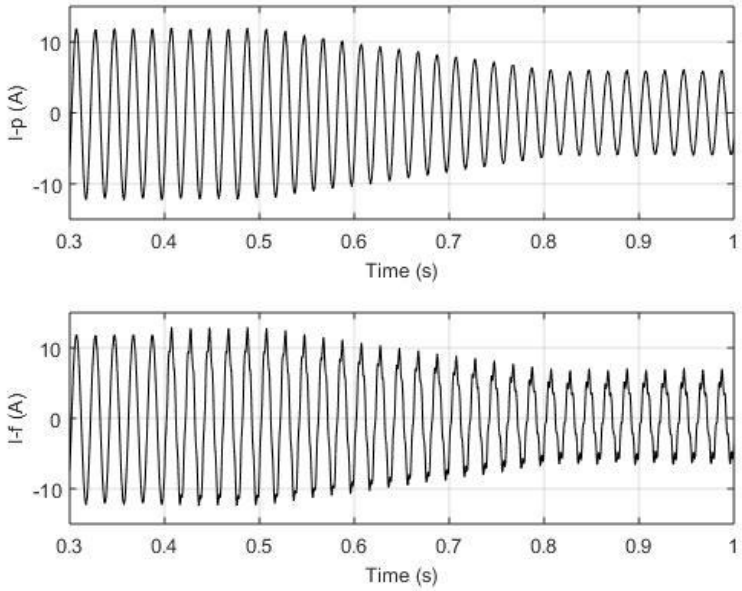


Figure 47: Results with no compensation implemented: primary current $I_p$, feeder Current $I_f$ [131].

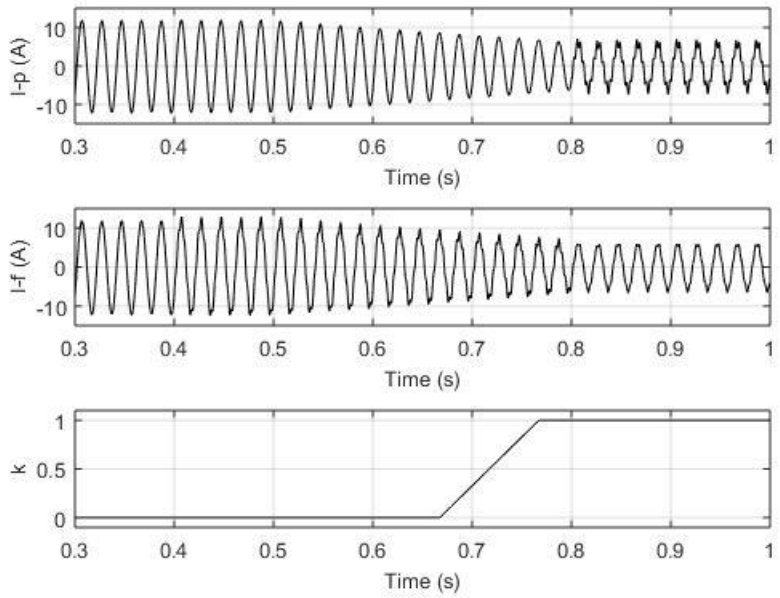


Figure 48: Results with no compensation implemented: PV inverter current $I_p$, source Current $I_f$ and harmonic current derating coefficient $k$ [131].

### 7.2.3 Simulation results for Example 3

The performance of the control algorithm presented in [113] is highlighted in this Section. The control system response is analysed for different load conditions, which are obtained by changing the firing angle (α) of thyristor-controlled load.

Figure 49 shows the source current (referred to as PCC current) without (a) and with (b) compensation under three different load scenarios. Initially, in both figures, the firing angle is set to α = 0°, then it is changed to 30° at t = 0.1 s and to 60° at t = 0.2 s. Figure 49 (a) shows that the source current is severely distorted for all three load scenarios. In Figure 49 (b), harmonic compensation is enabled and the source current appears to be sinusoidal with a small residual harmonic distortion. These graphs show that the control scheme is capable of injecting appropriate levels of harmonic current, as the load current changes (both current magnitude and harmonic content).

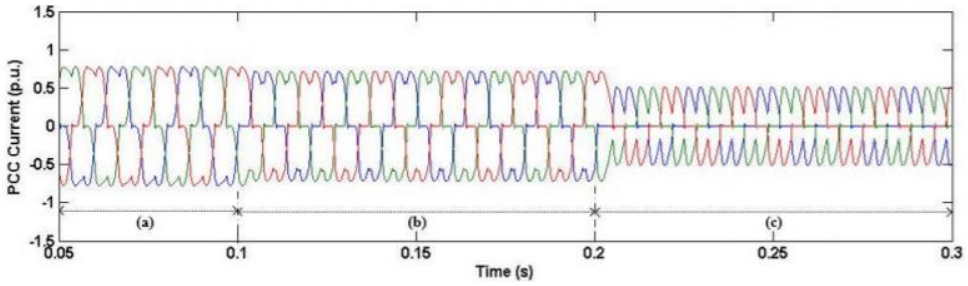


(a)

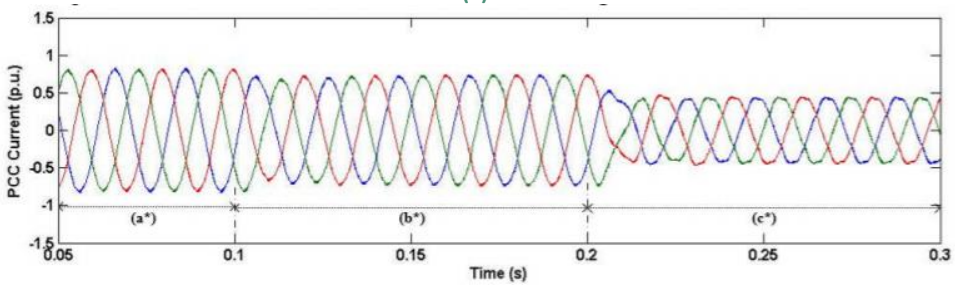


(b)

Figure 49: Source current waveform for varying firing angle α: (a) without and (b) with harmonic compensation enabled [116].

## 7.3 Previous hardware testing of combined AF/power converter concepts

Experimental results regarding the implementation of AF operation within multi-functional inverters are not very common in the literature review, partly due to the novelty of this approach[5]. However, two examples will be described in the following sections.

### 7.3.1 Experimental results for Example 3

Experimental results for a MMCC converter used as AF and unbalance compensator simultaneously are presented in [134]. The control system used in this work is similar to the one described in [113], but a notch filter is used instead of a LP filter for harmonic extraction.

Figure 50 shows the experimental results for this method. During the time interval between $0 < t < 0.1$ s, harmonic compensation is disabled, the source current $I_{sabc}$ is unbalanced and not in phase with the source voltage $V_{sabc}$ and distorted with harmonics. For $0.1 < t < 0.2$ s, the controller performs both reactive current compensation and harmonic current cancellation but does not balance the load current. The source current is therefore sinusoidal and in phase with the source voltage, but three phase values are unbalanced. The PV inverter terminal voltage and current ($V_{C\_abc}$ and $I_{C\_abc}$) are distorted since the controller injects harmonic currents. For $t > 0.2\ s$, the controller compensates the current unbalance by increasing the unbalance factor, while simultaneously supplying the load reactive current and harmonic compensation. As a result, the load current is well-balanced with a small residual harmonic distortion and in phase with the source voltage.

[5] Experimental results on stand-alone AF can be found in [138].

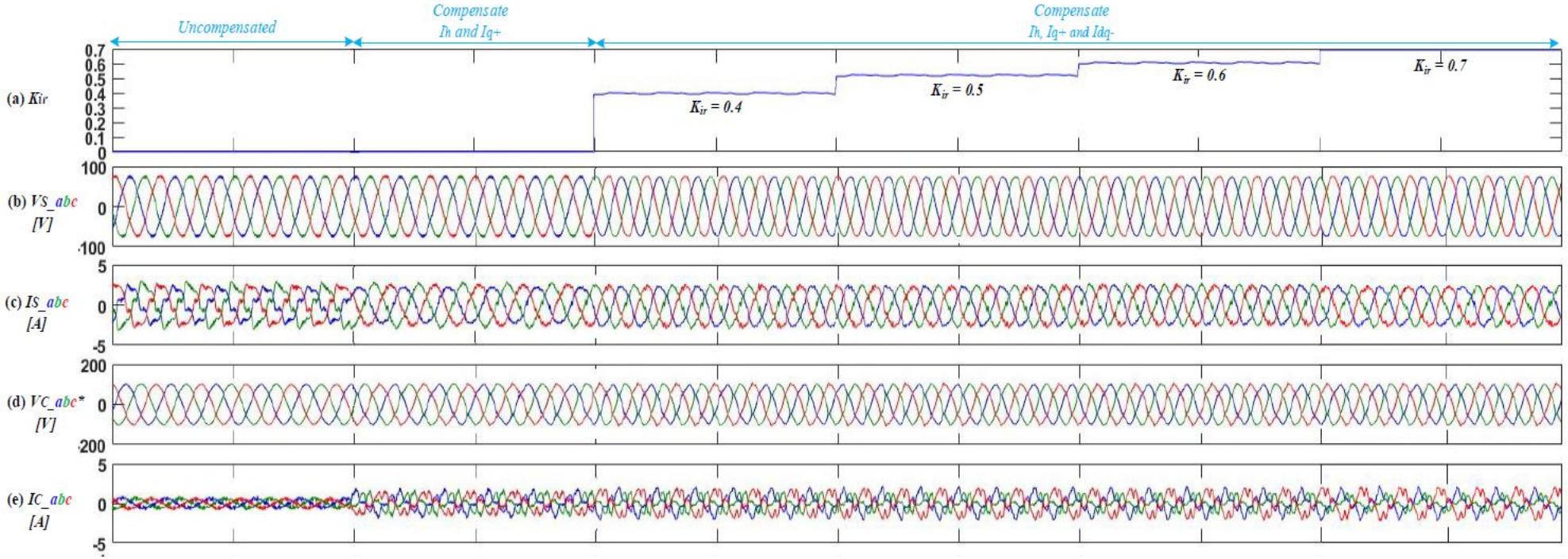


Figure 50: Compensation of both load current harmonics and imbalance [134].

### 7.3.2 Example 4: Multifunctional wind-PV system

An example of hardware implementation of multifunction inverter to mitigate harmonics and load unbalance is proposed in [132], where the authors present a multifunctional on-grid hybrid wind–PV system. The AF control method is based on the hysteresis controller for the inner current loop and a multistage adaptive filter (MAF) based control structure for fundamental and harmonics current extraction. The authors provide a similar work in [133], where a PV inverter (without wind generation) is used and a Kalman filter is implemented for harmonic extraction.

The experimental results under rated wind speed of 12 m/s and rated solar irradiation of 1000 W/m$^2$ are presented in Figure 51. A balanced non-linear load is connected to the PCC. The PCC voltage and load current are given in Figure 51 (a), the load power and load current THD are given in Figure 51 (b) - (c). The load current is a quasi-square waveform with amplitude of 4.289 A and 23.7% total harmonic distortion. The power demand of the local load is 1.56 kW.

Under these conditions, the PV inverter is controlled to operate as AF. The inverter terminal voltage, current and output power are shown in Figure 51 (d) and (e). The output current amplitude is 13.38 A and the active power delivered from the PV inverter is 5.08 kW. The output current is distorted because the inverter is injecting currents to compensate for the load harmonic distortion. The source current, source power and the source current harmonic spectrum are presented in Figure 51 (f)–(h). As a result of the PV inverter control, the source current observed is sinusoidal with amplitude of 9.19 A. The source current amplitude is lower than the current provided by the PV inverter because the latter is supplying the non-linear load. The surplus active power flowing to the source is 3.52 kW. The power factor at the source side is close to unity.

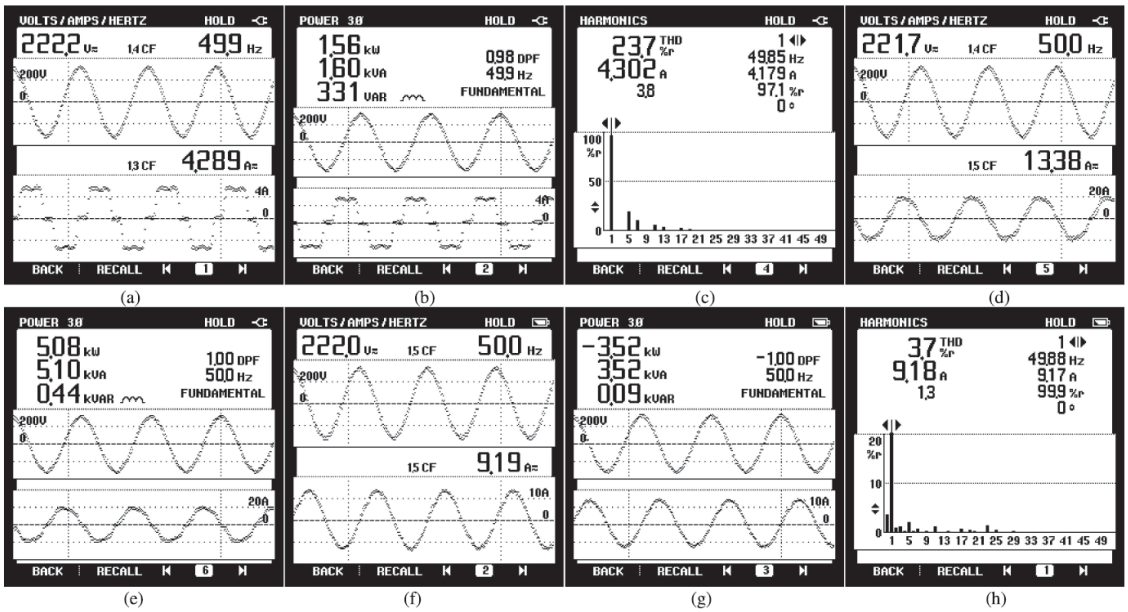


**Figure 51: Test results of a hybrid system at rated wind speed (12 m/s) and solar irradiation (1000 W/m2), (a) PCC voltage and current, (b) load power demand, (c) load current spectrum and THD, (d) PV inverter voltage and current, (e) PV inverter output power, (f) source voltage and current, (g) source power and (h) source current harmonic and THD [132].**

## 7.4 Example 5: Implementation of AF functionality in a STATCOM

A recent implementation of harmonic compensation has been performed in south-west Scotland, where existing STATCOMs have been upgraded to compensate for harmonics caused by nearby wind farms [130]. The region under consideration includes four wind farms connected in close proximity to a Line-Commutated Converter (LCC). As a result of harmonic pollution and resonance conditions, the voltage distortion at the 33 kV bus exceeded the planning levels (Table 1 and Table 4).

In order to mitigate this problem, the STATCOMs were programmed with upgraded control loops that enabled AF operation. The basic AF control configuration implemented in the Glenapp Wind Farm STATCOM is illustrated in Figure 52. In this case, voltage harmonics are accurately identified by the STATCOM Real Time Controller (RTC). Therefore, the STATCOM RTC was upgraded to detect the presence of 11$^{th}$ and 13$^{th}$ order voltage harmonics and continuously track their amplitude and phase angle. This was achieved through the utilization of an Advanced Adaptive Digital Filter [136].

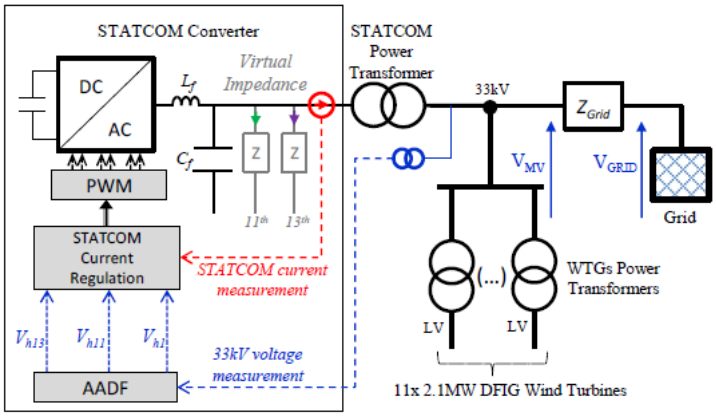


Figure 52: Overview of the control algorithm used to control the Glenapp Wind Farm STATCOM [130].

Grid voltage and STATCOM output currents are shown in Figure 53 for the case when AF operation was disabled. In this case, voltage THD was 3.3%. Figure 54 shows the results when AF operation is enabled: the addition of harmonic currents to the fundamental is visible. The voltage THD is then reduced to 1%.

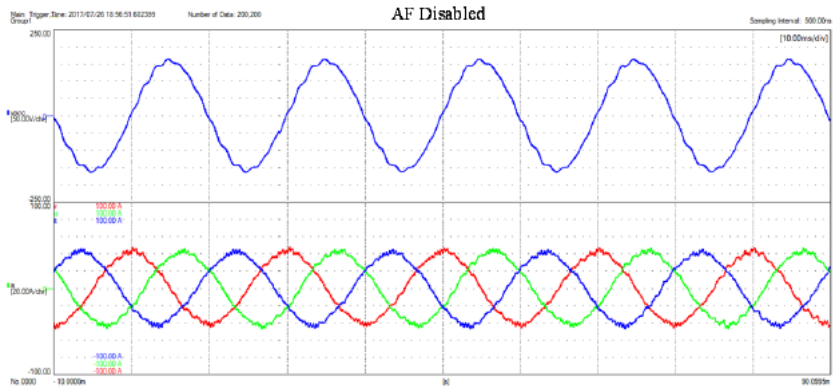


Figure 53: Measured grid phase voltage and STATCOM 3-phase output currents. AF disabled [130].

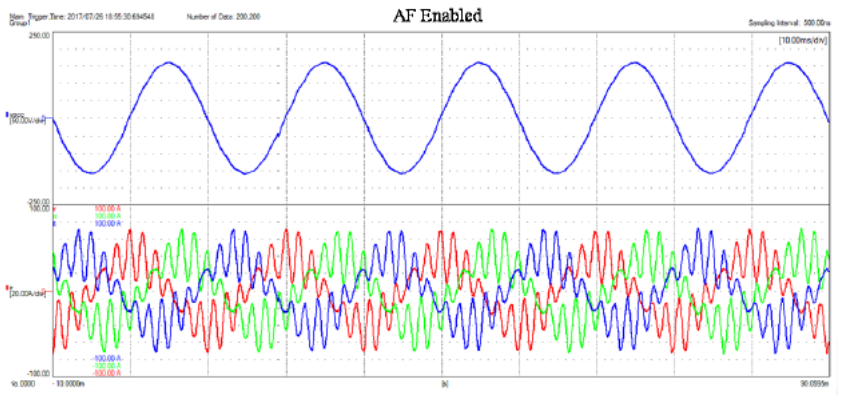


Figure 54: Measured grid phase voltage and STATCOM 3-phase output currents AF enabled [130].

## 7.5 Application proposed in this project

Consideration of the examples described in the previous sections allows us to draw the following conclusions:

- The use of multi-functional inverters as active filters results in a reduction of the harmonic content in the source current waveform, while the load current is not affected (Figure 46 for Example 1 and Figure 51 in Example 4);
- An harmonic derating coefficient is required to ensure that the inverter ratings is not exceeded when harmonic current components are injected simultaneously with fundamental power (Figure 42 for Example 1 and Figure 44 for Example 2);
- The majority of the projects found in the literature are based on harmonic current extraction, however, Example 5 shows that a STATCOM can be successfully deployed as AF by detecting harmonic voltages (Figure 52 for Example 5);
- Active filter operation is effective even when the load harmonic content is changing rapidly (Figure 49 for Example 3), since the response time of the inverter is in the order of milliseconds.

The main advantage of using power converters as active filters in addition to their core function of active power delivery is that no dedicated equipment for harmonic mitigation needs to be installed on the distribution grid. As a result, the following benefits can be identified:

- **No additional space is required in the substation or at customer premises** to implement harmonic mitigation. In some cases, in particular in thickly populated areas, the footprint required by harmonic mitigating solutions may be an important consideration in terms of feasibility.
- **The cost of this solution is limited when compared to installing dedicated Active Filters.** The graph shown in Figure 38 indicates that AFs are an expensive solution. When harmonic compensation is added to an existing converter, the implementation costs will be limited to software upgrade and inclusion of additional measurement ports. While these costs will be manufacturer-dependent, it can be estimated that they will be only a fraction of the total inverter cost (probably around 10-20%).

- **Potential revenue stream for the customers.** As described in the previous pages, PV inverters do not operate at full power for most of the time, either because of sun irradiance conditions (as shown in Figure 39), or because of curtailment. Therefore, the possibility of providing active filter functionality and delivering an ancillary service, may provide an additional source of income. The extent to which income from harmonic mitigation would economically incentivise a RES operator to de-load active power to allow harmonic filtering within device current limits is an open question.

These benefits lead to research and development activity in this area, which has been summarised in the previous paragraphs, in terms of control functionalities, simulation results, experimental tests and implementation. The results shown in Section 7.2 and in Section 7.3 demonstrate the technical feasibility of this method. The success of the project described in [130] demonstrates the use of power electronic converters to provide AF operation as an ancillary service is a mature technology.

Therefore, the proposed innovation project fits within an existing research activity aiming at developing new solutions for harmonic control, using assets that have already been installed on the grid.
The work proposed within this innovation project presents the following features:

- Consideration of the AF concept in a real 33 kV distribution system. As explained in Section 6.1, in most of the cases AF are applied at the low-voltage level. Additionally, in most of the cases, even when simulation results are presented, the system is modelled as a Thevenin equivalent. In contrast, within this project, the impact of the proposed application on a fully described 33 kV network will be considered in detail.
- Consideration of mitigating harmonics based on measurements at a point on the network remote from the power converter PCC.
- Implementation of a coefficient to limit harmonic injection when fundamental power flow from the PV inverter is above a threshold (where the threshold depends on both active power output and required harmonic injection). This will allow protecting the inverter from overrating.
- Coordination between PV inverters to ensure the most optimised operating condition is obtained, based on the operating point of each unit and the system network conditions.
- Validation of the proposed algorithm using hardware-in-the loop.

The control algorithm developed in this project will make use of some of the techniques described in Section 5 and in this section. Among the various methods described, the most suitable for the proposed application will be selected as the project develops.

# 8 Next steps

The next step of the project will consist in building a computer model of the power grid surrounding Tiverton bulk supply point. An overview of the area to be included in the model is shown in Figure 55. The main busbar at Tiverton is rated 33 kV and the substation is supplied by two 132/33 kV transformers.

Tiverton main busbar supplies eight 11 kV busbars (anticlockwise listing):

- Tiverton Moorhays (bus 7735)
- Tiverton South (bus 7737)
- Bridge Mills (bus 7117)
- Cullompton (bus 7236)
- Dunkeswell (bus 7271)
- Hemyock (bus 7367)
- Burlescombe (bus 7136)
- Tiverton Junction (bus 7733)

Note that the network includes: one radial feeder (Tiverton 33kV, Ayshford Court, Burlescombe, Hemyock, Dunkeswell);two ring circuits (Tiverton 33 kV, Tiverton Moorhays, Tiverton South and Tiverton 33kV), (Tiverton 33 kV, Cullompton Solar Park, Bridge Mills, Cullompton, Stoneshill SP, and Tiverton 33kV); plus Tiverton Junction, directly connected to the Tiverton 33kV bus.

Three solar farms exist within the 33 kV system, and these will be considered within the study: Ayshford Court (bus 9370), Stoneshill farm (bus 9850) and Cullompton (bus 9830).

The model will be developed in MATLAB and Simulink and validated against the following data:

- DIgSILENT PowerFactory model of the area
- Snapshot scenarios: Up to six different operating conditions will be studied. The operating scenarios will be based on scaling generation and load levels to match real operating conditions in the Western Power Distribution grid.
- Time series analysis: Half hour operating data will be used to assess the matching of the model with time-varying operating conditions.
- Harmonic measurements: voltage and current measurements have been taken at these locations: Tiverton BSP (8345/TIVE3), Ayshford Court (9370/AYSH3), Stoneshill Farm (9850/STFA3), Cullompton PV (9830/CMPV3).

A detailed description of the snapshot scenarios, time-series data, harmonic measurements, and model validation will be included in the next progress report.

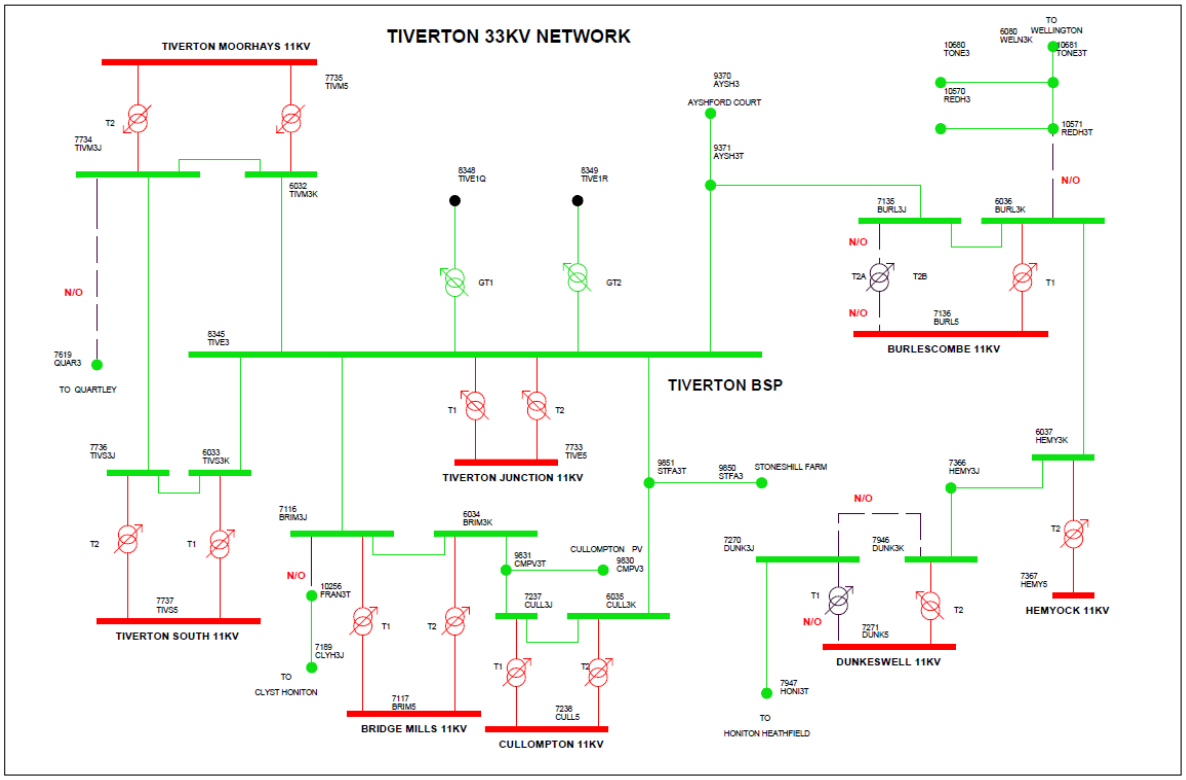


Figure 55: Tiverton Substation Area.

# 9 Conclusions

Due to the large number of power electronic-based devices installed in recent years, an increase of harmonic current and voltage levels on the power grid has been observed. Since harmonics can result in negative effects on power grid operation and on the power quality delivered to the customers, planning and operational codes require limitation of harmonic levels.

When harmonics levels are above prescribed emission limits specified in connection agreements, harmonic mitigations are required, and they can be broadly divided into passive filters and active filters. With the most recent advances of power electronics and controls, it is now possible to embed active filters as an 'ancillary service' with power converter units, thus avoiding the installation of dedicated devices.

The Harmonic Mitigation project will develop an active filter control algorithm for PV inverters installed within the Tiverton network, with the aim to identify the benefits and issues of this application.

# 10 Bibliography

[1] H. Akagi, "New trends in active power filters for power conditioning," *IEEE Transactions on Industry Applications,* vol. 32, no. 6, p. 1312–1322, 1996.

[2] J. P. M. Rocha, F. Salvadori and C. S. Gehrke, "Provision of ancillary service in a grid-connected photovoltaic power system," *2018 IEEE Applied Power Electronics Conference and Exposition (APEC), San Antonio, TX,* pp. 2355-2361, 2018.

[3] E. E. C. Morais, F. D. de A. Lima, J. M. L. Fonseca, C. G. C. Branco and L. de A. Machado, "Providing Ancillary Services with Wind Turbine Generators Based on DFIG with a Two-Branch Static Converter," *Energies,* vol. 12, 2019.

[4] M. Prodanovic, K. De Brabandere, J. Van Den Keybus, T. Green and J. Driesen, "Harmonic and reactive power compensation as ancillary services in inverter-based distributed generation," *in IET Generation, Transmission & Distribution,* vol. 1, no. 3, pp. 432-438, May 2007.

[5] J. Arrilaga and N. R. Watson, Power System Harmonics, 2nd Edition, Hoboken, NJ, John Wiley & Sons, 2003.

[6] The Electricity Council, "Engineering Recommendation G5/3, Limits for harmonics in the United Kingdom electricity supply system," 1976.

[7] IEEE Standards Association, "IEEE 519 - Recommended Practice and Requirements for Harmonic Control in Electric Power Systems," 2014.

[8] International Electrotechnical Commission, "IEC 61000-3-3, Electromagnetic compatibility (EMC) - Part 3-3: Limits - Limitation of voltage changes, voltage fluctuations and flicker in public low-voltage supply systems, for equipment with rated current ≤16 A per phase and not subject to conditional," 2013.

[9] The Energy Networks Association, "Engineering Recommendation G5/4-1: Planning Levels for Harmonic Voltage Distortion and the Connection of Non-Linear Equipment to Transmission Systems and Distribution Networks in the United Kingdom," 2005.

[10] Western Power Distribution, "Distribution System Operability Framework - Chapter 8: Power Quality," 2018.

[11] L. S. Czarnecki, "An overview of methods of harmonic suppression in distribution systems," *2000 Power Engineering Society Summer Meeting (Cat. No.00CH37134),* vol. 2, pp. 800-805, Seattle, WA, 2000.

[12] K. Al-Haddad, "Power quality issues under constant penetration rate of renewable energy into the electric network," *Proceedings of 14th International Power Electronics and Motion Control Conference EPE-PEMC 2010,* pp. S11-39-S11-49., Ohrid, 2010.

[13] Lee, H. J.; Nam, T.; Son, G.T; Park, J. W,; Chung, Y.H.; Lee, U.H.; Baek, S.T.; Hur, K.; , "Double-tuned filter design for HVDC system," *Transactions of the Korean Institute of Electrical Engineers,* vol. 61, no. 9, pp. 1232-1241, 2012.

[14] R. C. Duncan, M. F. McGranaghan, S. Santoso and W. Beaty, "Electrical Power Systems Quality," *McGraw-Hill,* p. 580, 2012.

[15] Y. Cho and H. Cha, "Single-tuned Passive Harmonic Filter Design Considering Variances of Tuning and Quality Factors," *Journal of International Council on Electrical Engineering,* vol. 1, no. 1, pp. 7-13, 2011.

[16] H. Fujita and H. Akagi, "A Practical Approach to Harmonic Compensation in Power Systems-Series Connection of Passive and Active Filters," *IEEE Transactions on Industry Applications,* vol. 27, no. 6, p. 1020 – 1025, Nov/Dec 1991.

[17] B. K. Bose, "Modern Power Electronics and AC drives," Prentice-Hall, 2002.

[18] S. Mikkili and A. K. and Panda, "Power quality issues: current harmonics," CRC press, 2015..

[19] H. Jou, J. Wu, Y. Chang, Y. Feng and W. Hsu, "New active power filter and control method," *in IEE Proceedings - Electric Power Applications,* vol. 152, no. 2, pp. 175-181, March 2005.

[20] A. R. Gothane, B. B. Baliwant and V. B. Waghmare, "Simulation and Analysis of Series Active Filter Using AC-AC Converter for Mitigation of Sag," *2019 3rd International Conference on Computing Methodologies and Communication,* pp. 886-889, India, 2019.

[21] Z. Wang, Q. Wang, W. Yao and J. Liu, "A series active power filter adopting hybrid control approach," *IEEE Transactions on Power Electronics,* vol. 16, no. 3, pp. 301-310, May 2001.

[22] L. Moran, P. Werlinger, J. Dixon and R. Wallace, "A series active power filter which compensates current harmonics and voltage unbalance simultaneously," *Proceedings of PESC '95 - Power Electronics Specialist Conference, Atlanta, GA, USA,* vol. 1, pp. 222-227, 1995.

[23] G. W. Chang and W. C. Chen, "A new reference compensation voltage strategy for series active power filter control," *IEEE Transactions on Power Delivery,* vol. 21, no. 3, pp. 1754-1756, July 2006.

[24] M. El-Habrouk, "A new configuration for shunt active power filters," *Electrical Engineering and Electronics Dept., Brunel University, PhD Thesis, ,* 1998.

[25] S. Rahmani, A. Hamadi, N. Mendalek and K. Al-Haddad, "A New Control Technique for Three-Phase Shunt Hybrid Power Filter," *IEEE Transactions on Industrial Electronics,* vol. 56, no. 8, pp. 2904 - 2915, 2009.

[26] P. C. Tan, A. Jusoh and Z. Salam, "A Single-Phase Hybrid Active Power Filter Connected to a Photovoltaic Array," *2006 3rd IET International Conference on Power Electronics, Machines and Drives - PEMD 2006,* pp. 85-89, The Contarf Castle, Dublin, Ireland, 2006.

[27] S. Rahmani, A. Hamadi, K. Al-Haddad and L. A. Dessaint, "A Combination of Shunt Hybrid Power Filter and Thyristor-Controlled Reactor for Power Quality," *IEEE Transactions on Industrial Electronics,* vol. 61, no. 5, pp. 2152-2164, May 2014.

[28] Y. Xu, X. Xiao, H. Liu and H. Wang, "Parallel operation of hybrid active power filter with passive power filter or capacitors," *2005 IEEE/PES Transmission & Distribution Conference & Exposition: Asia and Pacific, Dalian,* pp. 1-6, 2005.

[29] M. J. Newman and D. G. Holmes, "A universal custom power conditioner (UCPC) with selective harmonic voltage compensation," *IEEE 2002 28th Annual Conference of the Industrial Electronics Society. IECON 02,* vol. 2, pp. 1261-1266, Sevilla-2002.

[30] V. Khadkikar and A. Chandra, "A Novel Structure for Three-Phase Four-Wire Distribution System Utilizing Unified Power Quality Conditioner (UPQC)," *IEEE Transactions on Industry Applications,* vol. 45, no. 5, pp. 1897-1902, Sept.-oct. 2009.

[31] N. Singh and I. Thakur, "A review on power quality improvement in distribution system using UPQC," *International Journal of Engineering and Technology,* vol. 3, no. 7, p. 1253–1257, 2016.

[32] W. U. K. Tareen, M. Aamir, S. Mekhilef, M. Nakaoka, M. Seyedmahmoudian, B. Horan and N. A. Baig, "Mitigation of power quality issues due to high penetration of renewable energy sources in electric grid systems using three-phase APF/STATCOM technologies: A review," *Energies,* vol. 11, no. 6, p. 1491, 2018.

[33] H. Singh, M. Kour, D. Thanki and P. Kumar, "A Review on Shunt Active Power Filter Control Strategies," *International Journal of Engineering and Technology ,* vol. 7, p. 121–125, 2018.

[34] M. Diab, M. El-Habrouk, T. H. Abdelhamid and S. Deghedie, "Survey of Active Power Filters Configurations," *2018 IEEE International Conference on Systems, Computation, Automation and Networking (ICSCAN), Pondicherry, 2018,* pp. 1-14.

[35] W. M. Grady, M. J. Samotyj and A. H. Noyola, "Survey of active power line conditioning methodologies," *IEEE Transactions on Power Delivery,* vol. 5, no. 3, pp. 1536-1542, July 1990.

[36] L. A. Moran, J. W. Dixon and R. R. Wallace, "A three-phase active power filter operating with fixed switching frequency for reactive power and current harmonic compensation," *IEEE Transactions on Industrial Electronics,* vol. 42, no. 4, pp. 402-408, Aug 1995.

[37] H. Akagi, Y. Kanazawa and A. Nabae, “Instantaneous Reactive Power Compensators Comprising Switching Devices without Energy Storage Components,” *IEEE Transactions on Industry Applications,* Vols. IA-20, no. 3, pp. 625-630, May 1984.

[38] E. F. Couto, J. S. Martins and J. L. Afonso, “Simulation Results of a Shunt Active Power Filter with Control Based on p-q Theory,” *Proc. of International Conference on Renewable Energies and Power Quality (ICREPQ'03),* pp. 1-6, Vigo (Spain), April 2003.

[39] J. Liu, J. Yang and Z. Wang, “A new approach for single-phase harmonic current detecting and its application in a hybrid active power filter,” *IECON'99. Conference Proceedings. 25th Annual Conference of the IEEE Industrial Electronics Society (Cat. No. 99CH37029),* vol. 2, pp. 849-854, San Jose,CA,USA, 1999.

[40] R. S. Herrera, P. Salmeron and H. Kim, “Instantaneous reactive power theory applied to active power filter compensation: Different approches assessment and experimental results,” *IEEE Trans. Ind. Electron.,* vol. 55, no. 1 , pp. 184-196, Jan. 2008.

[41] K. V. Singh, P. Bhavsar and N. Patel, “Matlab simulation of single phase shunt active filter based on PQ theory,”,” *Int. J. Adv. Electr. Electron. Eng.,* vol. 3, no. 1, p. 56–65.

[42] R. H. Park, “Two-reaction theory of synchronous machines generalized method of analysis-part I,” *in Transactions of the American Institute of Electrical Engineers,* vol. 48, no. 3, pp. 716-727, July 1929.

[43] P. Mattavelli, “Synchronous frame harmonic control for highperformance Performance AC power supliers,” *IEEE Transaction of Industrial Applications,* vol. 37, no. 2, p. 864 –872, 2001.

[44] S. Bhattacharya and D. Divan, “Synchronous frame based controller implementation for a hybrid series active filter system,” *IAS '95. Conference Record of the 1995 IEEE Industry Applications Conference Thirtieth IAS Annual Meeting,* vol. 3, pp. 2531-2540, Orlando, FL, USA, 1995.

[45] H. J. Azevedo, J. M. Ferreira, A. P. Martins and A. S. Carvalho, “Directe Current Control of an Active Power Filter For Harmonic Elimination, Power Factor Correction and Load Unbalancing Compensation,” *Proceedings of the 10th European Conference on Power Electronics and Applications, EPE‟03,* pp. 1-10, Toulouse, 2003.

[46] S. Williams and R. Hoft, “Adaptive frequency domain control of PWM switched power line conditioner,” *IEEE Trans. Power Electron,* vol. 6, no. 4, p. 665 –670, 1991.

[47] H. S. Stone, “R66-50 An Algorithm for the Machine Calculation of Complex Fourier Series,” *in IEEE Transactions on Electronic Computers,* Vols. EC-154, pp. 680-681, Aug. 1966.

[48] G. Choe and M. Park, “Analysis and control of active power filter with optimized injection,” *IEEE Trans. Pow. Elect.,* pp. 427- 433, 1989.

[49] A. V. Oppenheim and A. S. Willsky, "Signals and Systems," *Prentice Hall, Upper Saddle River,* 1997.

[50] K. Borisov, H. Ginn and G. Chen, "A computationally efficient RDFT-based reference signal generator for active compensators," *IEEE Transactions on Power Delivery,* vol. 24, no. 4, pp. 2396- 2404, 2009.

[51] K. Borisov and H. Ginn, "A novel reference signal generator for active power filters based on recursive DFT," *In Twenty-Third Annual IEEE Applied Power Electronics Conference and Exposition,* pp. 1920-1925, 2008.

[52] L. Tey, P. So and Y. Chu, "Improvement of power quality using adaptive shunt active filter," *IEEE Transactions on power delivery,* vol. 20, no. 2, pp. 1558-1568, 2005.

[53] J. Barros and R. I. Diego, "Analysis of Harmonics in Power Systems Using the Wavelet-Packet Transform,," *in IEEE Transactions on Instrumentation and Measurement,* vol. 57, no. 1, pp. 63-69, Jan. 2008.

[54] M. Marinelli and L. Salvatore, "Wavelet-based algorithms Applied to harmonic detection for active shunt filters," *11th International Conference on Harmonics and Quality of Power 2004,Sept. 12-15, 2004,* 721 -727.

[55] D. Yazdani, A. Bakhshai and P. K. Jain, "A Three-Phase Adaptive Notch Filter-Based Approach to Harmonic/Reactive Current Extraction and Harmonic Decomposition," *IEEE Transactions on Power Electronics,* vol. 25, no. 4, pp. 914-923, April 2010.

[56] M. Rukonuzzaman and M. Nakaoka, "An advanced active power filter with adaptive neural network based harmonic detection scheme," *2001 IEEE 32nd Annual Power Electronics Specialists Conference,* vol. 3, pp. 1602-1607, Vancouver, BC, 2001.

[57] L. Tey and Y. Chu, "Adaptive neural network control of active filters," *Electric Power Systems Research, 2005.,* vol. 1, no. 74, pp. 37-56, 2005.

[58] Y. Qu, W. Tan, Y. Dong and Y. Yang, "Harmonic detection using fuzzy LMS algorithm for active power filter," *2007 International Power Engineering Conference (IPEC 2007),* pp. 1065-1069, Singapore, 2007.

[59] R. R. Pereira, C. H. da Silva, L. E. B. da Silva and G. Lambert-Torres, "Application of adaptive filters in active power filters," *2009 Brazilian Power Electronics Conference, Bonito-Mato Grosso do Sul,* pp. 770-774, 2009.

[60] F. Kamran and T. G. Habetler, "Combined deadbeat control of a series parallel converter combination used as a universal power filter," *in proceedngs of the 1995 IEEE/PELS Power Electronics Specialist Conference,* pp. 196-201, 1995.

[61] Z. Xie, Z. Liang, X. Wei and H. Zhang, "Energy Shaping Repetitive Control (ESRC) for Three-Phase Three-Wire Shunt Active Power Filter," *2009 Asia-Pacific Power and Energy Engineering Conference,* pp. 1-4, Wuhan, 2009.

[62] S. Fukuda, T. Kanayama and K. Muraoka, "SFX algorithm based adaptive control of active filters without detecting current harmonics," *Second International Conference on Power Electronics, Machines and Drives (PEMD 2004)., Edinburgh, UK, ,* vol. 1, pp. 258-264, 2004.

[63] E. Wiebe-Quintana, "Delta-Sigma Integral Sliding-Mode Control Strategy of a Three-Phase Active Power Filter using d-q Frame theory," *Electronics, Robotics and Automotive Mechanics Conference (CERMA'06),* pp. 291-298, Cuernavaca, 2006.

[64] S. K. Ram, S. R. Prusty, P. K. Barik, K. K. Mahapatra and B. D. Subudhi, "FPGA implementation of digital controller for active power line conditioner using SRF theory," *2011 10th International Conference on Environment and Electrical Engineering,* pp. 1-5, Rome, 2011.

[65] H.-S. Song and K. Nam, "Dual current control scheme for PWM converter under unbalanced input voltage conditions," *IEEE Transactions on Industrial Electronics,* vol. 46, no. 5, pp. 953-959, Oct 1999.

[66] Y. Suh and T. A. Lipo, "Control scheme in hybrid synchronous stationary frame for PWM AC/DC converter under generalized unbalanced operating conditions," *IEEE Transactions on Industrial Applicatons ,* vol. 42, no. 3, pp. 825-835, May-June 2006.

[67] M. Reyes, P. Rodriguez, S. Vazquez, A. Luna, J. M. Carrasco and R. Teodorescu, "Decoupled Double Synchronous Reference Frame current controller for unbalanced grid voltage conditions," in *IEEE Energy Conversion Congress and Exposition (ECCE)*, Raleigh, NC, , 15-20 Sept. 2012, pp. 4676-4682..

[68] P. Rodriguez, A. Luna, R. Teodorescu and F. Blaabjerg, "Grid Synchronization of Wind Turbine Converters under Transient Grid Faults using a Double Synchronous Reference Frame PLL," in *2008 IEEE Energy 2030 Conference, Atlanta, GA, 2008, pp. 1-8.*.

[69] I. Jeong, B. Johyon and K. Nam, "Dynamic modeling and control for SPMSMS with internal turn short fault," *IEEE Transaction on Power Electronics,* vol. 28, no. 7, p. 3495–3508, July 2013.

[70] A. H. Abosh and Z. Q. Zhu, "Current control of permanent magnet synchronous machine with asymmetric phases," *7th IET International Conference on Power Electronics, Machines and Drives (PEMD 2014), Manchester,* pp. 1-6, 2014.

[71] R. Ribeiro, T. Rocha, R. de Sousa, E. dos Santos and A. Lima, "A Robust DC-Link Voltage Control Strategy to Enhance the Performance of Shunt Active Power Filters Without Harmonic Detection Schemes," *IEEE Transactions on Industrial Electronics,* vol. 62, no. 2, pp. 803-813, Feb. 2015.

[72] N. Mendalek, K. Al-Haddad, F. Fnaiech and L. A. Dessaint, "Nonlinear control technique to enhance dynamic performance of a shunt active power filter," *in IEE Proceedings - Electric Power Applications,* vol. 150, no. 4, pp. 373-379, July 2003.

[73] A. P. Martins, "The Use of an Active Power Filter for Harmonic Elimination and Power Quality Improvement in a Nonlinear Loaded Electrical Installation," *Proceedings of the International Conference on Renewable Energies and Power Quality, ICREPQ'03,* pp. 1-6, Vigo, 2003.

[74] P. Dey and S. Mekhilef, "Current controllers of active power filter for power quality improvement: A technical analysis," *Journal for Control, Measurement, Electronics, Computing and Communications,* vol. 56, no. 1, p. 42–54, 2015.

[75] L. Malesani, P. Mattavelli and S. Buso, "Dead-Beat current control for active filters," *in Proceedings of the 24th Annual Conference of the IEEE Industrial Electronics Society, IECON '98, ,* p. 1859–1864., Aachen, Germany, 1998.

[76] L. Ge, X. Yuan and Z. Yang, "Control system design of shunt active power filter based on active disturbance rejection and repetitive control techniques," *Mathematical Problems in Engineering,* pp. 1-6, 2014.

[77] D. Chen and S. Xie, "Review of the control strategies applied to active power filters," *in IEEE International Conference on Electric Utility Deregulation, Restructuring and Power Technologies (DRPT2004), 2004,* p. 666–670.

[78] J. Miret, L. G. De Vicuna, M. Castilla, J. Cruz and J. M. Guerrero, "A simple sliding mode control of an active power filter," *in IEEE 35th Annual Power Electronics Specialisls Conference, Aachen, Germany, 2004,* p. 1052–1056.

[79] R. Hao, Z. Cheng and X. You, "A novel harmonic currents detection method based on rotating d-q reference frame for active power filter," *in 35th Annual IEEE Power Electronics Specialists Conference, Aachen, Germany, 2004,* p. 3034–3038.

[80] G. Adam, A. G. Stan and G. Livinţ, "An adaptive hysteresis band current control for three phase shunt active power filter using fuzzy logic," *in International Conference and Exposition on Electrical and Power Engineering (EPE 2012), Iasi, Romania,* pp. 324-329, 2012.

[81] Y. Han, L. Xu, M. M. Khan, G. Yao, L. Zhou and C. Chen, "Study on a novel approach to active power filter control using neural network-based harmonic identification scheme," *Springer, Electrical Engineering,* vol. 91, p. 313– 325, 2010.

[82] M. Cirrincione, M. Pucci, G. Vitale and G. Scordato, "A single-phase shunt active power filter for current harmonic compensation by adaptive neural filtering," *in 12th International Power Electronics and Motion Control Conference EPE-PEMC, Portoroz,* p. 1830–1835, Slovenia, 2006.

[83] T. Ponnusamy and Y. Narri, “Control of shunt active power filter using soft computing techniques,” *Journal of Vibration and Control,* vol. 20, no. 5, p. 713–723, 2014.

[84] A. Gligor, “Design and simulation of a shunt active filter in application for control of harmonic levels,” *Acta Universitatis Sapientiae Electrical and Mechanical Engineering, 1,* p. 53–63, 2009.

[85] H. Vahedi, A. A. Shojaei, L. Dessaint and K. Al-haddad, “Reduced dc link voltage active power filter using modified puc5 converter,” *IEEE Transactions on Power Electronics,* vol. 33, no. 2, pp. 943-947, Feb. 2017.

[86] R. Dian, W. Xu and C. Mu, “Improved negative sequence current detection and control strategy for h-bridge three-level active power filter,” *IEEE Transactions on Applied Superconductors,* vol. 26, no. 7, 2016.

[87] R. Dehini and S. Sefiane, “Power quality and cost improvement by passive power filters synthesis using ant colony,” *Journal of Theoretical and Applied Information Technology,* p. 70–79, 2011.

[88] A. K. Tiwari and S. P. Dubey, “Ant colony optimization based hybrid active power filter for harmonic compensation,” *in International Conference on Electrical, Electronics, and Optimization Techniques (ICEEOT), Chennai, India,,* p. 777–782, 2016.

[89] D. Chen and S. Xie, “Review of the control strategies applied to active power filters,” *in IEEE International Conference on Electric Utility Deregulation, Restructuring and Power Technologies (DRPT2004),,* vol. 2, p. 666–670, Hong Kong, China, 2004.

[90] M. El-Habrouk, M. K. Darwish and P. Mehta, “Active Power Filters : A Review,” *in IEE Proceedings - Electric Power Applications,* vol. 147, no. 5, p. 403–413, 2000.

[91] M. Ortuzar, R. Carmi, J. Dixon and L. Morán, “Voltage source active power filter, based on multi-stage converter and ultracapacitor dc-link.,” *in The 29th Annual Conference of the IEEE industrial Electronics Society (IECON), Roanoke,* pp. 2300-2305, USA, 2003.

[92] N. Vázquez, H. López, C. Hernández, E. Vázquez, R. Osorio and J. Arau, “A Different Multilevel Current-Source Inverter,” *IEEE Transactions Industrial Electronics,* vol. 57, no. 8, p. 2623–2632, 2010.

[93] G. K. Malla and A. Ramulu, “Simulation study of UPQC and active power filters for a Non-Linear Load,” *International Journal of Current Engineering and Technology,* vol. 5, no. 1, pp. 375–384,, 2015.

[94] J. Holtz, “Pulsewidth modulation for electronic power conversion,” in *Proceedings of the IEEE*, vol. 83, no. 8, Aug. 1994, pp. 1194-1214.

[95] A. M. Hava, R. J. Kerkman and T. A. Lipo, "A high performance generalized discontinuous PWM algorithm," *in IEEE Transactions on Industry Applications,* vol. 34, no. 5, pp. 1059-1071, Sept.-Oct. 1998.

[96] G. Narayanan and V. T. Ranganathan, "Extension of operation of space vector PWM strategies with low switching frequency using different overmodulation algorithms," *IEEE Transactions on Power Electronics ,* vol. 17, no. 5, p. 788–798, 2002.

[97] D. Lee and C. Lee, "A novel overmodulation technique for space-vector PWM inverters," *IEEE Transactions on Power Electronics,* vol. 13, no. 6, pp. 1144-1151, Nov, 1998.

[98] P. Kumar and A. Mahajan, "Soft Computing Techniques for the Control of an Active Power Filter," *in IEEE Transactions on Power Delivery,* vol. 24, no. 1, pp. 452-461, Jan. 2009.

[99] H. W. V. D. Broexk, H.-C. Skudelny and C. V. Stanke, "Analysis and realization of a pulse width modulator based on voltage space vector," *IEEE Transactions on Industry Applications,* vol. 24, p. 142–150, Jan./Feb. 1988.

[100] W. Zhang and Y.-H. Yu, "Comparison of Three SVPWM Strategies," Journal of electrical science and technology of China, vol. 5, no. 3, Sep. 2007.

[101] P. Xiao, G. Venayagamoorthy and K. Corzine, "Seven level shunt active power filter for high-power drive systems," *IEEE Transactions on Power Electronics,* vol. 24, pp. 6-13, 2009.

[102] N. Dai, M. Wong, F. Ng and Y. Han, "A FPGA-Based Generalized Pulse Width Modulator for Three-Leg Center-Split and Four-Leg Voltage Source Inverters," *IEEE Transactions on Power Electronics,* vol. 23, no. 3, pp. 1472-1484, May 2008.

[103] P. Henning, H. Fuchs, R. A.D. and H. D. T. Mouton, "A 1.5-MW Seven-Cell Series-Stacked Converter as an Active Power Filter and Regeneration Converter for a DC Traction Substation," *IEEE Transactions on Power Electronics,* vol. 23, no. 5, pp. 2230-2236, Sept. 2008.

[104] K. M. Rahman, M. R. Khan and M. A. Choudhury, "Implementation of programmed modulated carrier HCC based on analytical solution for uniform switching of voltage source inverters," *IEEE Transactions on Power Electronics,* vol. 18, no. 1, pp. 188-197, January 2002.

[105] G. H. Bode and D. G. Holmes, "Load independent hysteresis current control of three level single phase inverter with constant switching frequency," *2001 IEEE 32nd Annual Power Electronics Specialists Conference (IEEE Cat. No.01CH37230),* vol. 1, pp. 14-19, Vancouver, BC, 2001.

[106] NANCAL Technology Product List - Active Power Filter, "http://en.nancal.com/power-quality/active-power-filters.html," Accessed on 11/11/2019.

[107] M. Welsh, P. Mehta and M. Darwish, "Genetic algorithmal and extended analysis optimisation techniques for switched capacitor active filters - a comparative study," *IEE Proceedings-Electric Power Applications,* vol. 147, no. 1, pp. 21-26, 2000.

[108] J. Enslin and J. Van Wyk, "Measurement and compensation of fictitious power under nonsinusoidal voltage and current conditions," *IEEE Transactions on Instrumentation and Measurement,* vol. 37, no. 3, pp. 403-408, 1988.

[109] H. Jou, "Performance comparison of the three phase active power filter algorithms," *IEE Proc. Generation, Transmission and Distribution,* vol. 142, no. 6, pp. 646-652, 1995.

[110] H. Fujita, "Combined rectifying system including double-series capacitor-smoother diode rectifier and series active filter," *IEE Japan,* vol. 120, no. 1, pp. 85-94, 1997.

[111] G. D. P. Ledwich, "Multiple converter performance and active filtering," *IEEE Transactions on Power Electronics,* vol. 10, no. 3, pp. 273-279, 1995.

[112] J. Chen and X. Yuan, "Chain circuit active power filter for high voltage high power applications," *2014 17th International Conference on Electrical Machines and Systems (ICEMS),* pp. 2422-2425, Hangzhou, 2014.

[113] H. Huang, O. J. K. Oghorada, L. Zhang and B. P. Chong, "Active harmonic current elimination and reactive power compensation using modular multilevel cascaded converter," in *19th European Conference on Power Electronics and Applications (EPE'17 ECCE Europe)*, Warsaw, Poland , IEEE, 2017.

[114] V. Corasaniti, M. B. Barbieri, P. L. Arnera and M. I. and Valla, "Active and hybrid filters in medium voltage distribution power systems," *In Conseil International des Grands Réseaux Electriques (CIGRE) Session,* París, Francia, 2010.

[115] J. H. R. Enslin and J. D. Van Wyk, "A new control philosophy for power electronic converters as fictitious power compensators," *IEEE Trans. Pow. Elec.,* vol. 5, no. 1, pp. 88-97, 1990.

[116] G. L. Van Harmelen and J. H. R. Enslin, "Real-time dynamic control of dynamic power filters in supplies with high contamination," *in IEEE Transactions on Power Electronics,* vol. 8, no. 3, pp. 301-308, 1993.

[117] O. P. Singh, "Cost-benefit Analysis of Harmonic Current Reduction in PV System -A Review," *Journal of Basic and Applied Engineering Research,* vol. 4, no. 3, pp. 267-275, April-June, 2017.

[118] A. F. Zobaa and S. H. E. Abdel Aleem, "A New Approach for Harmonic Distortion Minimization in Power Systems Supplying Nonlinear Loads," *in IEEE Transactions on Industrial Informatics,* vol. 10, no. 2, pp. 1401-1412, May 2014.

[119] C. Kawann and A. E. Emanuel, "Passive shunt harmonic filters for low and medium voltage: a cost comparison study," *in IEEE Transactions on Power Systems,* vol. 11, no. 4, pp. 1825-1831, Nov. 1996.

[120] D. J. Carnovale, T. J. Dionise and T. M. Blooming, "Price and performance considerations for harmonic colutions," 29 5 2012. [Online]. Available: https://www.newark.com/pdfs/techarticles/eaton/Eaton_Technical_Articles/Power_Quality_White_Papers/Harmonic_Solutions.pdf. [Accessed 10 10 2019].

[121] Energy UK, "Ancillary services report," 01 04 2017. [Online]. Available: https://www.energy-uk.org.uk/publication.html?task=file.download&id=6138. [Accessed 15 12 2019].

[122] G. Verbic and F. Gubina, "Ancillary services management in the Slovenian power system," *IEEE Power Engineering Society Summer Meeting,* vol. 3, pp. 1656-1660, Chicago, IL, USA, 2002.

[123] E. Sortomme and M. A. El-Sharkawi, "Optimal scheduling of vehicle-to-grid energy and ancillary services," *IEEE Transactions on Smart Grid,* vol. 3, no. 1, pp. 351-359, March 2012.

[124] R. M. Domingos, L. S. Xavier, A. F. Cupertino and H. A. Pereira, "Current control strategy for reactive and harmonic compensation with dynamic saturation," *2015 IEEE 24th International Symposium on Industrial Electronics (ISIE),* pp. 669-674, Buzios, 2015.

[125] H. A. Pereira, R. M. Domingos, L. S. Xavier, A. F. Cupertino, V. F. Mendes and J. O. S. Paulino, "Adaptive saturation for a multifunctional three-phase photovoltaic inverter," *2015 17th European Conference on Power Electronics and Applications (EPE'15 ECCE-Europe),* pp. 1-10, Geneva, 2015.

[126] B. K. Perera, P. Ciufo and S. Perera, "Point of common coupling (PCC) voltage control of a grid-connected solar photovoltaic (PV) system," *IECON 2013 - 39th Annual Conference of the IEEE Industrial Electronics Society,* pp. 7475-7480, Vienna, 2013.

[127] L. S. Xavier, A. F. Cupertino and P. H. A. A., "Ancillary services provided by photovoltaic inverter:single and three phase control strategies," *Computer and electrical engineering,* vol. 70, pp. 102-121, 2018.

[128] Z. Yao and L. Xiao, "Control of Single-Phase Grid-Connected Inverters With Nonlinear Loads," *in IEEE Transactions on Industrial Electronics,* vol. 60, no. 4, pp. 1384-1389, April 2013.

[129] G. Todeschini and A. E. Emanuel, "Transient response of a wind energy conversion system used as active filter," *IEEE Transactions on Energy Conversion,* vol. 26, no. 2, pp. 522-531, 2010.

[130] J. C. P. Campion, E. O. Oregi and C. E. T. Foote, "Active Harmonic Filtering in STATCOMs for Enhanced Renewable Energy Integration," *Presented at IEEE ECCE Conference, Baltimore MD, 29 Sept-3,* Oct 2019..

[13 1] G. Todeschini, “Control and derating of a PV inverter for harmonic compensation,” Portland, USA, 2017, IEEE Power & Energy Society General Meeting.

[13 2] S. Pradhan, S. Murshid, B. Singh and B. K. Panigrahi, “Performance Investigation of Multifunctional On-Grid Hybrid Wind–PV System With OASC and MAF-Based Control,” *IEEE Transactions on Power Electronics,* vol. 34, no. 11, pp. 1808-1822, 2019.

[13 3] N. Kumar, B. Singh, B. K. Panigrahi, C. Chakraborty, H. M. Suryawanshi and V. Verma, “Integration of Solar PV With Low-Voltage Weak Grid System: Using Normalized Laplacian Kernel Adaptive Kalman Filter and Learning Based InC Algorithm,” *IEEE Transactions on Power Electronics,* vol. 34, no. 11, pp. 10746-10755, 2019.

[13 4] H. Huang, L. Zhang, O. Oghorada and M. Mao, “A delta-connected MMCC-based Active Power Conditioner for Unbalanced Load Compensation and Harmonic Elimination,” *International Journal of Electrical Power and Energy System,* vol. 118, pp. 1-15, 2020.

[13 5] N. Pogaku and T. Green, “Harmonic mitigation throughout a distribution system: a distributed-generator-based solution,” *IEE Proceedings on Generation, Transmission and Distribution,* vol. 153, no. 3, pp. 350-358, 2006.

[13 6] A. Bhattacharya and C. Chakraborty, “Predictive and Adaptive ANN (Adaline) Based Harmonic Compensation for Shunt Active Power Filter,” in *2008 IEEE Region 10 and the Third international Conference on Industrial and Information Systems*, Kharagpur, India, 2008.

[13 7] C. L. Phillips, J. M. Parr and E. A. Riskin, “Signals, Systems and Transforms,” *Prentice Hall,* p. 765, 2003.

[13 8] R. Balasubramanian, K. Parkavikathirvelu, R. Sankaran and K. Amirtharajan, “Design, Simulation and Hardware Implementation of Shunt Hybrid Compensator Using Synchronous Rotating Reference Frame (SRRF)-Based Control Technique,” *MPDI Electronics,* vol. 8, no. 42, pp. 1-20, 2019.